© 2021. Published by The Company of Biologists Ltd | Journal of Cell Science (2022) 135, jcs258336. doi:10.1242/jcs.258336

RESEARCH ARTICLE

SPECIAL ISSUE: CELL BIOLOGY OF LIPIDS

# Septins coordinate cell wall integrity and lipid metabolism in a sphingolipid-dependent process

**Alexander Mela* and Michelle Momany‡**

## ABSTRACT

Septins colocalize with membrane sterol-rich regions and facilitate recruitment of cell wall synthases during wall remodeling. We show that null mutants missing an *Aspergillus nidulans* core septin present in hexamers and octamers (Δ*aspA*$^{cdc11}$, Δ*aspB*$^{cdc3}$ or Δ*aspC*$^{cdc12}$) are sensitive to multiple cell wall-disturbing agents that activate the cell wall integrity MAPK pathway. The null mutant missing the octamer-exclusive core septin (Δ*aspD*$^{cdc10}$) showed similar sensitivity, but only to a single cell wall-disturbing agent and the null mutant missing the noncore septin (Δ*aspE*) showed only very mild sensitivity to a different single agent. Core septin mutants showed changes in wall polysaccharide composition and chitin synthase localization. Mutants missing any of the five septins resisted ergosterol-disrupting agents. Hexamer mutants showed increased sensitivity to sphingolipid-disrupting agents. Core septins mislocalized after treatment with sphingolipid-disrupting agents, but not after ergosterol-disrupting agents. Our data suggest that the core septins are involved in cell wall integrity signaling, that all five septins are involved in monitoring ergosterol metabolism, that the hexamer septins are required for sphingolipid metabolism and that septins require sphingolipids to coordinate the cell wall integrity response.

**KEY WORDS: Septins, MAPK signaling, Cell wall integrity, Sterol-rich domains**

## INTRODUCTION

The cell wall and plasma membrane (PM) are the primary lines of defense against environmental insults for fungal cells. With the large surface area of hyphal networks and intimate contact with the surrounding media, fungi encounter many stresses, ranging from ion imbalance to predation. The cell wall contains several polysaccharide constituents – chitin provides the rigid framework of the cell wall, β-glucan maintains the shape and mannans form the outermost, protective layer (Bulawa et al., 1995; Munro and Gow, 2001; Orlean, 2012; Schmidt, 2004; Shaw et al., 1991; Sudoh et al., 2000). Precise regulation of cell wall and plasma membrane architecture is attained by tightly coordinated signaling pathways, which control genes responsible for maintaining homeostasis between the intracellular and extracellular environments.

Septins are highly conserved small GTPase cytoskeletal proteins that function as molecular scaffolds for dynamic cell wall and plasma membrane-remodeling, as well as diffusion barriers restricting movement of membrane and cell wall-associated molecules (Caudron and Barral, 2009; Dobbelaere and Barral, 2004; Gladfelter et al., 2001; Glomb and Gronemeyer, 2016; Longtine and Bi, 2003; Oh and Bi, 2011; Takizawa et al., 2000; Trimble and Grinstein, 2015). The *Saccharomyces cerevisiae* septins Cdc3, Cdc10, Cdc11 and Cdc12 have been termed 'core septins' because they are monomers that assemble into non-polar heterooligomers and micrometer-scale higher order structures in the form of bars, rings or gauzes (Bertin et al., 2008; McMurray et al., 2011; McMurray and Thorner, 2019; Sirajuddin et al., 2007). *Aspergillus nidulans* contains four orthologous septin proteins – AspA$^{Cdc11}$, AspB$^{Cdc3}$, AspC$^{Cdc12}$ and AspD$^{Cdc10}$, as well as AspE, which has no *S. cerevisiae* ortholog (Pan et al., 2007). *A. nidulans* contains two distinct subpopulations of heterooligomers – an octameric oligomer consisting of all four core septins in the same order as proposed in *S. cerevisiae* (AspA$^{Cdc11}$–AspC$^{Cdc12}$–AspB$^{Cdc3}$–AspD$^{Cdc10}$–AspD$^{Cdc10}$–AspB$^{Cdc3}$–AspC$^{Cdc12}$–AspA$^{Cdc11}$), and a second hexameric oligomer, with the proposed order (AspA$^{Cdc11}$–AspC$^{Cdc12}$–AspB$^{Cdc3}$–AspB$^{Cdc3}$–AspC$^{Cdc12}$–AspA$^{Cdc11}$) (Glomb and Gronemeyer, 2016; Hernandez-Rodriguez et al., 2014; Oh and Bi, 2011). For clarity, we will refer to AspA$^{Cdc11}$, AspB$^{Cdc3}$ and AspC$^{Cdc12}$ as 'core hexamer septins'; AspA$^{Cdc11}$, AspB$^{Cdc3}$, AspC$^{Cdc12}$ and AspD$^{Cdc10}$ as 'core octamer septins'; and AspE as the 'noncore septin' because it does not assemble into oligomeric structures, though it is required for higher order structure assembly at the multicellular stage (Hernandez-Rodriguez et al., 2012, 2014).

Previous studies in *Candida albicans* have shown that septins provide the scaffolding for cell wall proteins via the cell wall integrity (CWI) mitogen-activated protein kinase (MAPK) signaling pathway (Blankenship et al., 2010; Caudron and Barral, 2009; Fukuda et al., 2009; Gladfelter et al., 2001; Mostowy and Cossart, 2012). The CWI pathway, along with the other major MAPK signaling pathways [high osmolarity glycerol (HOG), cAMP-protein kinase A (PKA), target of rapamycin (TOR), calcineurin/$Ca^{2+}$ and mating/pheromone response pathways] are highly conserved across the kingdom Fungi, and have been shown to undergo extensive cross-talk to coordinate virtually all biological functions in the cell, from expansion and division to asexual reproduction (Colabardini et al., 2014; Fujioka et al., 2006; Garcia et al., 2017; Manfiolli et al., 2019; Munro et al., 2007; Rodriguez-Pena et al., 2010; Walker et al., 2008; Wiederhold et al., 2005).

Sphingolipids are long chain base-containing lipids (Dickson, 2008) that are metabolized in a highly conserved pathway in plants, animals and fungi; sphingolipid metabolism shares direct connections to other major metabolic pathways, such as sterol metabolism and fatty acid and phospholipid synthesis (Sims et al., 2004). Sphingolipid pathway intermediates, such as phytosphingosine (PHS), have been shown to be involved in CWI

Fungal Biology Group and Plant Biology Department, University of Georgia, 2502 Miller Plant Science Building, Athens, GA 30602, USA.
*Present address: Department of Plant & Microbial Biology, University of California, Berkeley, CA 94712, USA.

‡Author for correspondence (mmomany@uga.edu)

M.M., 0000-0001-7110-063X

**Handling Editor: James Olzmann**
**Received 17 December 2020; Accepted 31 December 2020**

Journal of Cell Science (2022) 135, jcs258336. doi:10.1242/jcs.258336

pathway signaling in *S. cerevisiae* (Dickson, 2008; Roelants et al., 2002). Sterol-rich domains (SRDs), also called 'lipid rafts' or 'lipid microdomains', are regions of the plasma membrane enriched in specific classes of lipids, including sterols [ergosterol, the major sterol found in most fungi (Weete et al., 2010)], sphingolipids and phosphoinositides (Alvarez et al., 2007; Tanaka and Tani, 2018), which have been shown to be functionally important for maintenance of cell polarity (Bagnat and Simons, 2002). Membrane organization, plasticity and overall integrity have been attributed to sphingolipid, sterol and glycerophospholipid interactions (van Meer et al., 2008). *In vitro* work has shown that yeast septins bind directly to the phosphoinositides phosphatidylinositol 4,5-bisphosphate [PIP2 or PI(4,5)P2], phosphatidylinositol 5-phosphate [PI(5)P] and phosphatidylinositol 4-phosphate [PI(4)P] (Bertin et al., 2010; Krokowski et al., 2018; Tanaka-Takiguchi et al., 2009; Zhang et al., 1999). Septins have also been shown to genetically interact with Sur2, a sphinganine C4-hydroxylase which catalyzes the conversion of sphinganine to PHS in sphingolipid biosynthesis (Costanzo et al., 2010), and to physically interact with GTPases, Bud1 and Cdc42 to maintain sphingolipid-dependent diffusion barriers at cell membranes in yeast (Clay et al., 2014). Interdependent colocalization of septins and sterol rich microdomains have been described in a number of *in vivo* and *in vitro* systems (Beh et al., 2009; Martin and Konopka, 2004). In the dimorphic fungus *Ustilago maydis*, septins and SRDs depend on each other to localize properly at the hyphal tip for cell signaling and cell polarity establishment (Canovas and Perez-Martin, 2009). In the budding yeast *S. cerevisiae*, long-chain sphingolipids have been implicated in maintaining asymmetric distribution and mobility of some membrane-spanning molecules, such as multidrug resistance transporters (Singh et al., 2017). In contrast to these findings, a more recent comprehensive study of protein segregation during cell division in budding yeast found that the majority of endoplasmic reticulum (ER) and PM proteins with transmembrane domains were actually symmetrically segregated; however, septins were shown to be responsible for partitioning of the PM-associated ER at the bud neck, thereby restricting diffusion of ER lumen and a particular set of membrane-localized proteins (Sugiyama and Tanaka, 2019).

Recent work has started to unravel the functional connections between the septins, CWI MAPK pathway signaling and lipid metabolism; however, most studies have focused on a small subset of septin monomers and/or were conducted primarily in yeast-type fungi (Badrane et al., 2016; Bridges and Gladfelter, 2015; de Almeida, 2018; Merlini et al., 2015; Wu et al., 2010; Zhang et al., 2017). Here, we show in the filamentous fungus *A. nidulans* that the core septins AspA$^{Cdc11}$, AspB$^{Cdc3}$, AspC$^{Cdc12}$ and AspD$^{Cdc10}$ are required for proper coordination of the CWI pathway, that all five septins are involved in lipid metabolism and that these roles require sphingolipids.

## RESULTS

### Mutants missing core septins are sensitive to cell wall-disturbing agents and the mutant missing the noncore septin AspE is mildly sensitive to a single agent

To determine whether *A. nidulans* septins are important for CWI, we used spore dilution assays to test the growth of septin deletion mutants on medium containing a variety of known cell wall-disturbing agents. Wild-type (WT) and septin-null mutants were tested on Calcofluor White (CFW) and Congo Red (CR), cell wall polymer-intercalating agents that perturb chitin and β-1,3-glucan, respectively, as well as caspofungin (CASP), an inhibitor of β-1,3-glucan synthase, and fludioxonil (FLU), a phenylpyrrol fungicide that antagonizes the group III histidine kinase in the osmosensing pathway and consequently affects CWI pathway signaling (Fig. 1) (Dongo et al., 2009; Hohmann, 2002; Kojima et al., 2006; Kopecka and Gabriel, 1992; Kovacs et al., 2013; Kuranda et al., 2006; Onishi et al., 2000; Pancaldi et al., 1984; Roncero and Duran, 1985; Yun et al., 2014). Septin mutants Δ*aspA*$^{cdc11}$, Δ*aspB*$^{cdc3}$ and Δ*aspC*$^{cdc12}$ showed hypersensitivity to CFW, CR, CASP and FLU; Δ*aspD*$^{cdc10}$ displayed no sensitivity to CFW, CR and FLU, but sensitivity to CASP (see Table S1 for list of strains used in this study). The ΔaspE mutant showed no sensitivity to CFW, CASP and FLU, and very mild sensitivity to CR (Fig. 1A).

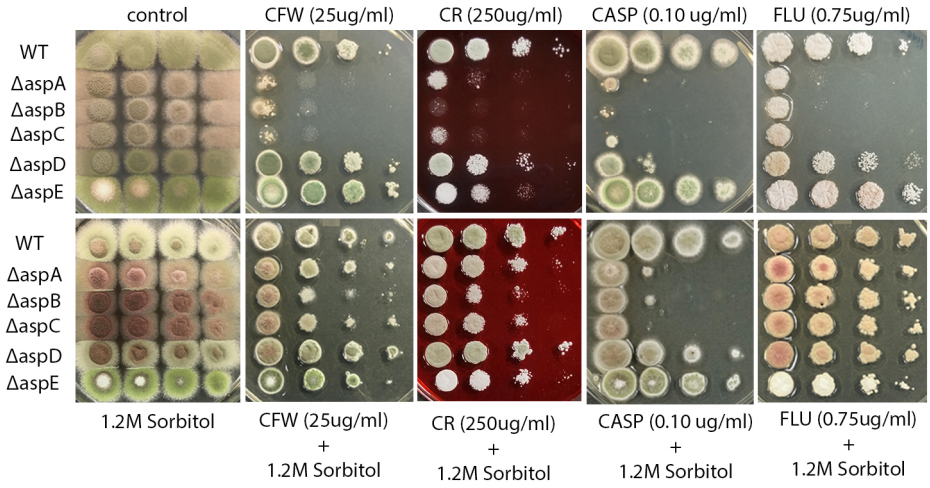


**Fig. 1. Septin-null mutants exhibit sensitivity to cell wall-disturbing agents, which can be rescued by osmotic support.** Top row, solid medium spotting assay. WT and septin-null mutants Δ*aspA*$^{cdc11}$, Δ*aspB*$^{cdc3}$, Δ*aspC*$^{cdc12}$, Δ*aspD*$^{cdc10}$ and Δ*aspE* were tested for sensitivity by spotting decreasing spore concentrations on complete medium plates with or without the cell wall-disturbing agents Calcofluor White (CFW), Congo Red (CR), caspofungin (CASP) and fludioxonil (FLU) at the indicated final concentrations. Bottom row, WT and septin-null mutants were tested for osmotic remediation of hypersensitivity to cell wall-disturbing agents, by spotting decreasing spore concentrations on media as in the top row but supplemented with exogenous 1.2 M sorbitol. Spore concentrations were between $10^7$ conidia/ml and $10^4$ conidia/ml for all assays. Differences in colony color result from changes in spore production, spore pigment and production of secondary metabolites under stress. The experiment was repeated five times with similar results.

Journal of Cell Science (2022) 135, jcs258336. doi:10.1242/jcs.258336

### Septin mutant sensitivity to cell wall-disturbing agents is rescued by osmotic stabilization

One hallmark of CWI defects is that they can be rescued by the addition of an osmotic stabilizer, such as sorbitol or sucrose. The addition of exogenous 1.2 M sorbitol partially rescued the hypersensitivity to CASP and fully rescued the hypersensitivity to CFW, CR and FLU for Δ*aspA*$^{cdc11}$, Δ*aspB*$^{cdc3}$ and Δ*aspC*$^{cdc12}$ (Fig. 1B). Sorbitol also rescued the sensitivity of Δ*aspD*$^{cdc10}$ to CASP and the mild sensitivity of Δ*aspE* to CR. The osmotic rescue of growth defects in the mutants indicates that their sensitivity to cell wall-disturbing agents is likely the result of a CWI defect.

### The core septin-null mutant Δ*aspB*$^{cdc3}$ has altered chitin and β-1,3-glucan localization

Because the core septin mutants showed sensitivity to cell wall-disturbing agents, consistent with action via the CWI pathway, we predicted that there might be differences in cell wall polymer localization in the mutants. To examine cell wall polymer localization, we undertook live-cell imaging of WT and Δ*aspB*$^{cdc3}$ since it is a member of both hexamers and octamers. Conidia were incubated on coverslips in liquid medium, stained with CFW or Aniline Blue to observe chitin and β-1,3-glucan, respectively, and immediately observed by fluorescence microscopy. *Z*-stack images were analyzed one-by-one, compressed into maximum projection images to visualize the fluorescence signal in the entire hyphal structure, and by line scans of Aniline Blue and CFW staining patterns (Fig. 2; Fig. S1). As previously reported, Δ*aspB*$^{cdc3}$ cells showed more presumptive branch initials per hyphal compartment than WT cells (Hernandez-Rodriguez et al., 2012). The Aniline Blue staining showed a reduction of labeling at all Δ*aspB*$^{cdc3}$ hyphal tips. Smaller patches of less intense Aniline Blue labeling also occurred at presumptive branch initials in Δ*aspB*$^{cdc3}$ than in WT (Fig. 2A; Fig. S1A). The CFW staining of Δ*aspB*$^{cdc3}$ showed a shift of the tip band of staining closer to the hyphal apex and a less well-defined endocytic collar zone than in WT (Fig. 2B; Fig. S1B). These data show that cell wall organization is altered in Δ*aspB*$^{cdc3}$ and raise the possibility that it might be altered in other core hexamer septin-null mutants as well.

### The core septin-null mutant Δ*aspB*$^{cdc3}$ has higher levels of chitin

Previous studies have shown that perturbations to one cell wall component often trigger compensatory changes to others via the CWI pathway (Fortwendel et al., 2010; Garcia-Rodriguez et al., 2000; Walker et al., 2008). To analyze the cell wall composition of septin mutants, two independent biological replicates of a diagnostic glycosyl linkage analysis (Pettolino et al., 2012) were conducted to quantify the cell wall polysaccharide composition of WT, Δ*aspB*$^{cdc3}$ (a core septin-null mutant which showed hypersensitivity to cell wall-disturbing agents) and Δ*aspE* (non-core septin mutant) (Fig. S2). All samples contained 3- and 4-linked glucose as the primary cell wall components, as well as 4-linked N-acetylglucosamine (the monomer of chitin; 4-GlcNAc) and a relatively minor amount of mannan. The septin mutants Δ*aspB*$^{cdc3}$ and Δ*aspE* showed 7% and 2% increases in the average area of the detected linkage peak for 4-GlcNAc compared to WT, respectively; the amount of 4-Glc and of mannan (data not shown) did not show significant differences between samples. These data indicate an increase in chitin content of the Δ*aspB*$^{cdc3}$ mutant and raise the possibility that it might be altered in other core hexamer septin-null mutants as well.

### Chitin synthase localization is altered in the core septin-null mutant Δ*aspA*$^{cdc11}$

Membrane-spanning cell wall synthases are the ultimate effectors of the CWI pathway. *A. nidulans* contains six genes for chitin synthases – *chsA*, *chsB*, *chsC*, *chsD*, *csmA* and *csmB*. Chitin synthase B localizes to sites of polarized growth in hyphal tips, as well as developing septa in vegetative hyphae and conidiophores, a pattern very similar to septin localization. Deletion of chitin synthase B causes severe defects in most filamentous fungi analyzed thus far, and repression of the chitin synthase B gene expression in *chsA*, *chsC* and *chsD* double mutants exacerbates growth defects from a number of developmental states observed in each single mutant, suggesting it plays a major role in chitin synthesis at most growth stages (Fukuda et al., 2009). For

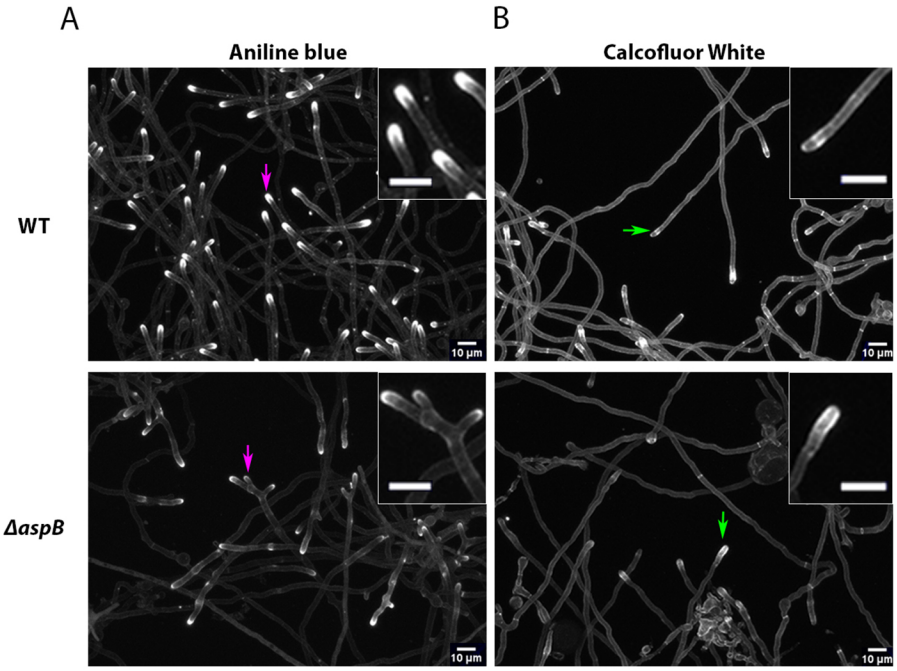


**Fig. 2. Cell wall staining reveals unique patterns of chitin and β-1,3-glucan deposition in the core septin hexamer null mutant Δ*aspB*$^{cdc3}$.** (A) WT and Δ*aspB*$^{cdc3}$ cells were incubated for ∼14 h and (A) stained with Aniline Blue to visualize β-1,3-glucan or (B) stained with Calcofluor White (CFW) to visualize chitin. Representative images are shown from at least three independent biological replicates, with ≥100 cells observed each. Magenta arrows in A denote hyphal tips with representative β-1,3-glucan deposition. Green arrows in B denote hyphal tips with representative chitin deposition. Insets show enlargement of area around the arrows. Scale bars: 10 µm. The experiment was repeated three times with similar results.

Journal of Cell Science (2022) 135, jcs258336. doi:10.1242/jcs.258336

these reasons, we chose chitin synthase B as a candidate to observe in a septin mutant background for possible defects in localization. We hypothesized that recruitment or maintenance of cell wall synthases, such as chitin synthase could be disrupted in septin-null mutants that showed sensitivity to cell wall-disturbing agents and altered cell wall staining patterns. To determine the localization of synthases, a chitin synthase B–GFP (*chsB-GFP*) strain was crossed with strains in which core hexamer septins were deleted. After repeated attempts, the only successful cross was with core hexamer deletion strain Δ*aspA*$^{cdc11}$. The Δ*aspA*$^{cdc11}$, *chsB-GFP* strain showed conspicuous differences in chitin synthase localization patterns compared to WT (Fig. 3; Fig. S3). In WT, the chitin synthase–GFP signal was at the tips of >90% of branches, presumptive branch initials and apical hyphal tips (Fig. S3A). In the septin-null mutant Δ*aspA*$^{cdc11}$, GFP signal was absent in most presumptive branch initials, but present in longer side branches that were at least 10 µm long and in the apical hyphal tip(s) (Fig. 3; Fig. S3A). Intriguingly, the chitin label CFW was more intense in the septin deletion strain, consistent with the increase in 4-GlcNAc levels seen in polysaccharide analysis (Fig. S3B). CFW labeling also showed that the polymer chitin was present throughout the hyphae in both the WT and septin deletion strains (Fig. 2) suggesting that chitin synthases had been active in both, but perhaps were not retained as long in the presumptive branch initials of the septin deletion mutant. These data support the hypothesis that core hexamer septins play a role in recruitment and/or retention of cell wall synthases to the proper locations at the plasma membrane during growth and development.

### Double-mutant analyses suggest that the core septin *aspB*$^{cdc3}$ modulates the CWI pathway in the Δ*mpkA* background under cell wall stress

To determine whether there are genetic interactions between the septins and the CWI pathway kinases, double mutants were generated by means of sexual crosses and analyzed. The first CWI pathway kinase, PkcA$^{Pkc1}$ (ANID_00106), is essential in *A. nidulans*, and so null alleles could not be utilized for double-mutant analysis. A null allele of the final kinase in the CWI MAPK signaling cascade, MpkA$^{Slt2}$ (ANID_11786), was crossed with Δ*aspB*$^{cdc3}$ and Δ*aspE*, and progeny were challenged with cell wall-disturbing treatments. If the septins were directly in the CWI pathway, we would expect double mutants to show the same phenotypes as the parental null mutant that acts earliest. If the septins were part of a parallel pathway or alternate node that also affected CWI, we would expect a novel or synergistic phenotype in the double mutants.

Spore dilution assays were conducted, challenging the double mutants and the parental strains with cell wall-disturbing treatments. The double mutants Δ*aspB*$^{cdc3}$Δ*mpkA*$^{slt2}$ and Δ*aspE* Δ*mpkA*$^{slt2}$ displayed a colony-level radial growth defect and reduced conidiation, which phenocopied the Δ*mpkA*$^{slt2}$ single mutant. When challenged with low concentrations of CASP and CFW, the Δ*aspB*$^{cdc3}$Δ*mpkA*$^{slt2}$ and Δ*aspE* Δ*mpkA*$^{slt2}$ mutants were more sensitive than Δ*aspB*$^{cdc3}$ and Δ*aspE* single mutants, but suppressed the colony growth defects of Δ*mpkA*$^{slt2}$. The novel phenotype of the double mutants shows that septins are involved in CWI and raises the possibility that they act in a bypass or parallel node for rescue of cell wall defects (Fig. 4).

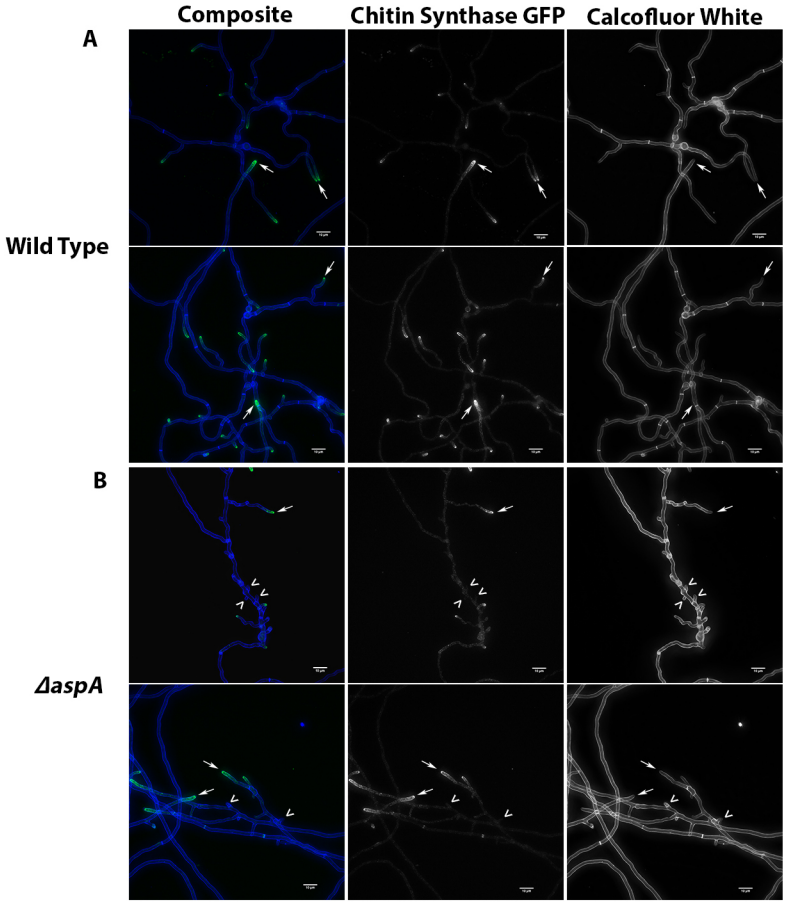


**Fig. 3. Chitin synthase is mislocalized in the core septin-null mutant Δ*aspA*$^{cdc11}$.** (A) Chitin synthase B–GFP in WT background (left and middle columns). (B) Chitin synthase B–GFP in a Δ*aspA*$^{cdc11}$ mutant background (left and middle columns). Calcofluor White labeling in A and B shows the presence of the polymer chitin at septa, main hyphal tips, branches and putative branch initials (right-hand column). Representative images are shown from at least three independent biological replicates, with ≥100 cells observed. White arrows highlight hyphal branches and tips. White arrowheads highlight putative branch initials. Scale bars: 10 µm. The experiment was repeated three times with similar results.

Journal of Cell Science (2022) 135, jcs258336. doi:10.1242/jcs.258336

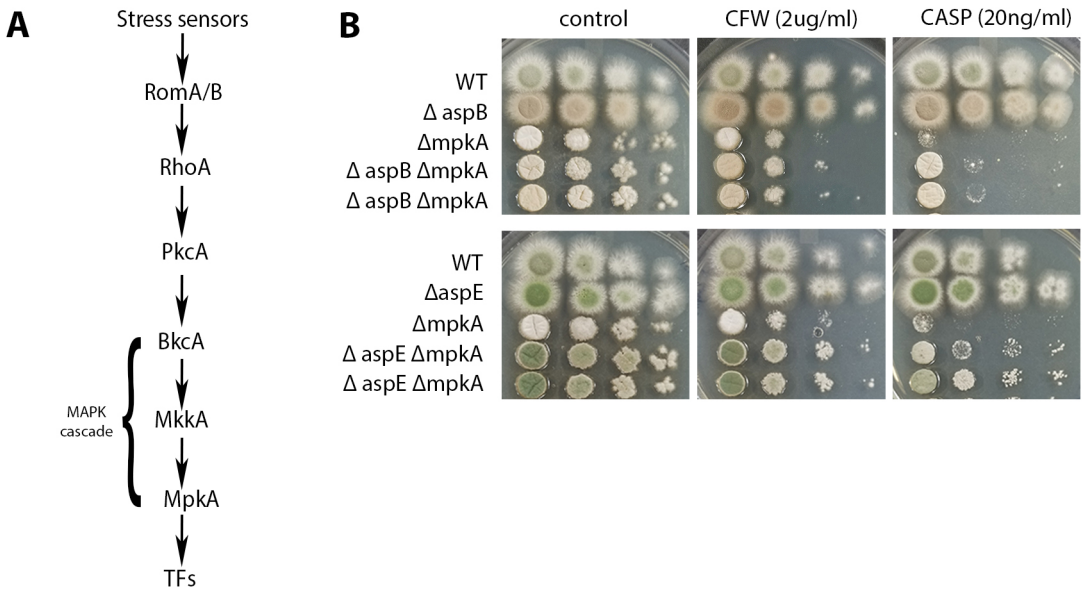


**Fig. 4. Double mutant analyses suggest core septins modulate the CWI pathway.** (A) Simplified schematic diagram of the *A. nidulans* CWI MAPK signaling pathway (Yoshimi et al., 2016). (B) Solid medium spotting assays. Top, WT, Δ*aspB*$^{cdc3}$, Δ*mpkA*$^{slt2}$ and two Δ*aspB*$^{cdc3}$Δ*mpkA*$^{slt2}$ double mutant strains were tested for sensitivity by spotting decreasing spore concentrations on complete medium plates with or without cell wall-disturbing agents. Bottom, WT, Δ*aspE*, Δ*mpkA*$^{slt2}$ and two Δ*aspE*Δ*mpkA*$^{slt2}$ double mutant strains were tested for sensitivity by spotting decreasing spore concentrations on complete medium plates with or without cell wall-disturbing agents. Differences in colony color result from changes in spore production, spore pigment and production of secondary metabolites under stress. TFs, transcription factors; CFW, Calcofluor White; CASP, caspofungin. Spore concentrations were between $10^6$ conidia/ml and $10^3$ conidia/ml for all assays in the figure. The experiment was repeated three times with similar results.

### Core septin-null mutants are insensitive to disruption of the $Ca^{2+}$/calcineurin, cAMP-PKA or TOR pathways, and Δ*aspE* is sensitive to some TOR pathway inhibitors

One possible explanation for the observed sensitivity to cell wall-disturbing agents could be that septins are involved in 'cross-talk' with other MAPK signaling pathways that have been shown to interact with the CWI pathway signaling such as the $Ca^{2+}$/calcineurin (CAMK) signaling pathway. To test this possibility, calcium chloride, EGTA (a $Ca^{2+}$-chelating agent) and FK-506 (a calcineurin inhibitor) were added to each treatment (Fig. S4) (Sio et al., 2005; Wang et al., 2016; Yoshimoto et al., 2002). The treatments caused no obvious colony growth defects, suggesting that the $Ca^{2+}$/calcineurin signaling pathway crosstalk does not significantly contribute to the observed sensitivity of septin-null mutants to cell wall-disturbing agents.

Another pathway closely associated with CWI, lipid biosynthesis and lipid signaling is the TOR MAPK signaling pathway (Harvald et al., 2015). To test the involvement of septins in this signaling pathway, septin-null mutants were challenged with rapamycin (a potent inhibitor of the TOR pathway), as well as the methylxanthine derivatives caffeine and theophylline (Barbet et al., 1996; Cardenas et al., 1999; Scott and Lawrence, 1998). There were no observable growth defects in the presence of rapamycin (final concentration was 600 ng/ml, which is ∼3-fold higher than the inhibitory concentration for known TOR pathway mutants) in the septin-null mutants compared to WT (Fig. S4) (Fitzgibbon et al., 2005; Soulard et al., 2010). Caffeine and theophylline have been shown to interfere with phosphodiesterase activity in the cAMP-PKA and TOR pathways, and Δ*pkaA*$^{tpk1}$ and Δ*tor1*$^{torA}$ mutants show hypersensitivity to caffeine treatment, which cannot be rescued by exogenous sorbitol (Binder et al., 2010; Butcher and Potter, 1972; Kuranda et al., 2006; Ni et al., 2005; Scott and Lawrence, 1998). If the septins were involved in crosstalk between the cAMP-PKA or TOR pathways and the CWI pathway, we would predict that septin-null mutants would be hypersensitive to caffeine and theophylline treatments. To our surprise, only Δ*aspE* showed hypersensitivity to both caffeine and theophylline, and the hypersensitivity was not rescued by an osmotic stabilizer (Fig. S4 and data not shown). These data suggest that the TOR, cAMP-PKA and $Ca^{2+}$/calcineurin signaling pathways do not contribute to the cell wall sensitivity or plasma membrane resistance phenotypes in the core septin-null mutants, but the cAMP-PKA or TOR pathways may contribute to the phenotypes of the septin Δ*aspE* null mutant.

### Core septin-null mutants show increased resistance to disruption of ergosterol biosynthesis and Δ*aspA*$^{cdc11}$ and Δ*aspE* show increased resistance to the ergosterol-binding drug natamycin

We hypothesized that septins could indirectly modulate MAPK pathways, particularly the CWI pathway, through interactions with plasma membrane lipids within SRDs. Recent work has shown that the CWI pathway in *S. cerevisiae* is regulated by sphingolipids and ergosterol, facilitating proper deposition of cell wall polymers at actively growing regions and sites of septation (de Almeida, 2018; Tanaka and Tani, 2018). It is well-established that septins localize to sites of polarized growth and septation, where highly dynamic remodeling of the plasma membrane and cell wall via membrane-bound synthases and polarity-associated proteins takes place (Foderaro et al., 2017). These highly dynamic plasma membrane SRDs in fungi often contain ergosterol and sphingolipids. To determine whether loss of septins might affect one of the major SRD-associated lipids, each septin mutant was challenged by drug treatments disrupting the ergosterol biosynthesis pathway in spore dilution assays (Fig. 5). These assays included an azole treatment (itraconazole), an allylamine treatment (terbinafine), and a polyene treatment (natamycin), which each impact a different step in ergosterol biosynthesis (Fig. 5A). Allylamines (terbinafine) inhibit the conversion of squalene to squalene epoxide, azoles

Journal of Cell Science (2022) 135, jcs258336. doi:10.1242/jcs.258336

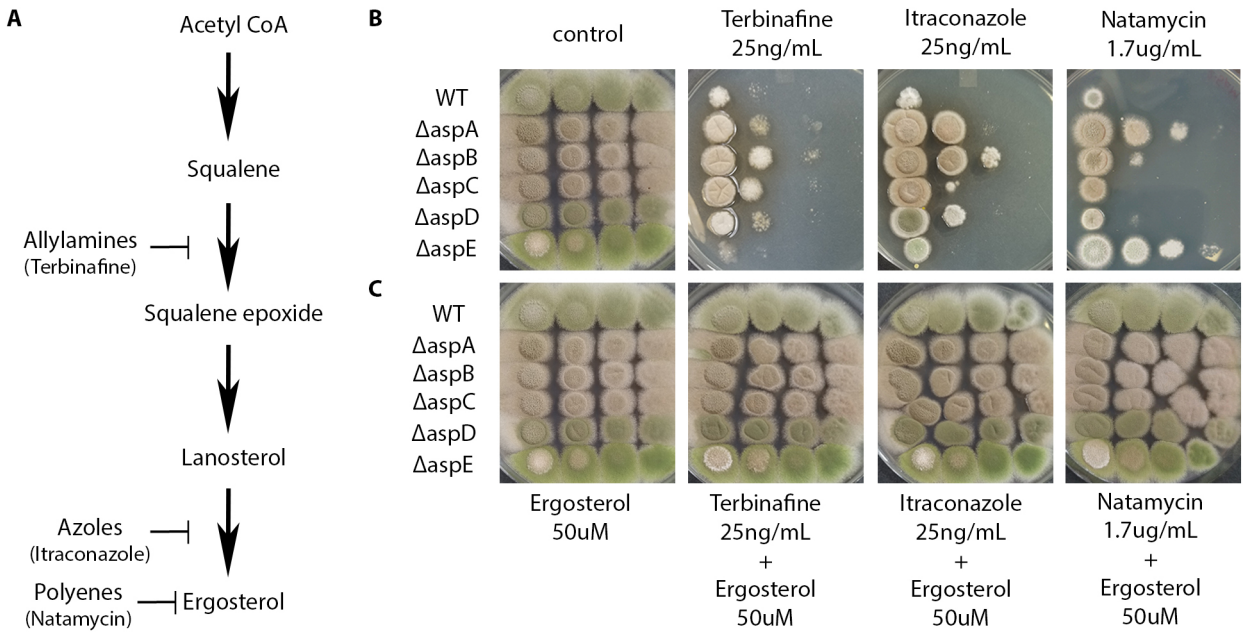


**Fig. 5. Core septin-null mutants show increased resistance to disruption of ergosterol biosynthesis and Δ*aspA*$^{cdc11}$ and Δ*asp*E show increased resistance to the ergosterol-binding polyene drug natamycin.** (A) A simplified schematic diagram of the ergosterol biosynthesis pathway, showing where allylamines, azoles and polyene antifungal agents affect each step (Onyewu et al., 2003). (B) WT and septin-null mutants Δ*aspA*$^{cdc11}$, Δ*aspB*$^{cdc3}$, Δ*aspC*$^{cdc12}$, Δ*aspD*$^{cdc10}$ and Δ*aspE* were tested for sensitivity by spotting decreasing spore concentrations on solid medium with or without the ergosterol biosynthesis-disturbing agents terbinafine, itraconazole and natamycin at the concentrations shown. (C) Rescue of sensitivity to ergosterol biosynthesis-inhibiting treatments. WT and septin-null mutants were tested for the ability of exogenous ergosterol (50 µM) to rescue sensitivity to ergosterol biosynthesis-disturbing agents. Differences in colony color result from changes in spore production, spore pigment and production of secondary metabolites under stress. Spore concentrations were between $10^7$ conidia/ml and $10^4$ conidia/ml for all assays in the figure. The experiment was repeated three times with similar results.

(itraconazole) inhibit the conversion of lanosterol to 4,4-dimethylcholesta-8,14,24-trienol, and polyenes bind directly to ergosterol (Onyewu et al., 2003).

The Δ*aspA*$^{cdc11}$, Δ*aspB*$^{cdc3}$, Δ*aspC*$^{cdc12}$ and Δ*aspD*$^{cdc10}$ mutants were more resistant to itraconazole and terbinafine than WT or Δ*aspE*. Only Δ*aspA*$^{cdc11}$ and Δ*aspE* showed strong resistance to natamycin treatment (Fig. 5B). The addition of exogenous 50 µM ergosterol was able to fully rescue the sensitivity of all null mutant strains and WT to itraconazole, terbinafine and natamycin, suggesting ergosterol was indeed the primary lipid component disrupted by these treatments (Fig. 5C). These data suggest that all five septins are involved in monitoring ergosterol metabolism and/or deposition.

### Core hexamer septin-null mutants show altered sensitivity to disruption of sphingolipid biosynthesis

Sphingolipids are a class of plasma membrane lipids that has been shown to be associated with SRDs, along with sterols and phosphoinositides, and therefore are possible targets for septin-mediated interactions at the membrane. To determine whether loss of septins impacts sphingolipid metabolism in *A. nidulans*, the septin-null mutants were challenged with sphingolipid biosynthesis-disrupting agents myriocin and aureobasidin A (AbA) (Fig. 6). Myriocin disrupts the first committed step of the biosynthetic pathway, converting palmitoyl-coA and serine into 3-ketodihydrosphingosine, preventing the accumulation of downstream intermediates, such as ceramides and sphingoid bases like PHS, as well as complex sphingolipids at the final steps of the pathway (Fig. 6A) (Alvarez et al., 2007; Martin and Konopka, 2004). Aureobasidin A inhibits IPC synthase, disrupting the conversion of inositolphosphorylceramide from phytoceramide, and consequently causing the accumulation of intermediates such as PHS, which has been shown to be toxic at high concentrations (Fig. 6A) (Cheng et al., 2001).

The core hexamer null mutants Δ*aspA*$^{cdc11}$, Δ*aspB*$^{cdc3}$ and Δ*aspC*$^{cdc12}$ were more sensitive to myriocin than the other septin-null mutant or WT cells (Fig. 6B). Δ*aspA*$^{cdc11}$, Δ*aspB*$^{cdc3}$ and Δ*aspC*$^{cdc12}$ were also more resistant to AbA than null mutants of the octamer-exclusive septin Δ*aspD*$^{cdc10}$, the noncore septin Δ*aspE* or WT (Fig. 6B). Strikingly, the addition of exogenous PHS (15 µM) to the myriocin treatment fully rescued the sensitivity of Δ*aspA*$^{cdc11}$, Δ*aspB*$^{cdc3}$ and Δ*aspC*$^{cdc12}$ (Fig. 6C). Δ*aspA*$^{cdc11}$, Δ*aspB*$^{cdc3}$ and Δ*aspC*$^{cdc12}$ were also more resistant to higher concentrations (20 µM) of the phytosphingosine intermediate (PHS), which has been shown to be toxic at high concentrations (Fig. 6C) (Li et al., 2007).

To address whether cell wall and plasma membrane defects might be associated with one another in septin-null mutants, a combinatory drug treatment approach was taken. Sublethal concentrations of CFW (2 µg/ml) and myriocin (10 µg/ml), in which all strains grew at every spore concentration, were combined (Fig. 6D). When combined, the two drugs resulted in additive, colony-level growth defects for Δ*aspA*$^{cdc11}$, Δ*aspB*$^{cdc3}$ and Δ*aspC*$^{cdc12}$. This sensitivity to both drugs in combination was rescued by the addition of exogenous PHS. Surprisingly the addition of exogenous sorbitol, which had fully rescued the hypersensitivity of the septin-null mutants to all previously tested cell wall-disturbing agents, resulted in a more dramatic growth defect in medium containing only myriocin, or in combination with CFW (Fig. 6C,D). These data together suggest that the core hexamer septins AspA$^{Cdc11}$, AspB$^{Cdc3}$ and AspC$^{Cdc12}$ may monitor sphingolipid metabolism. They further suggest that the hexamer

Journal of Cell Science (2022) 135, jcs258336. doi:10.1242/jcs.258336

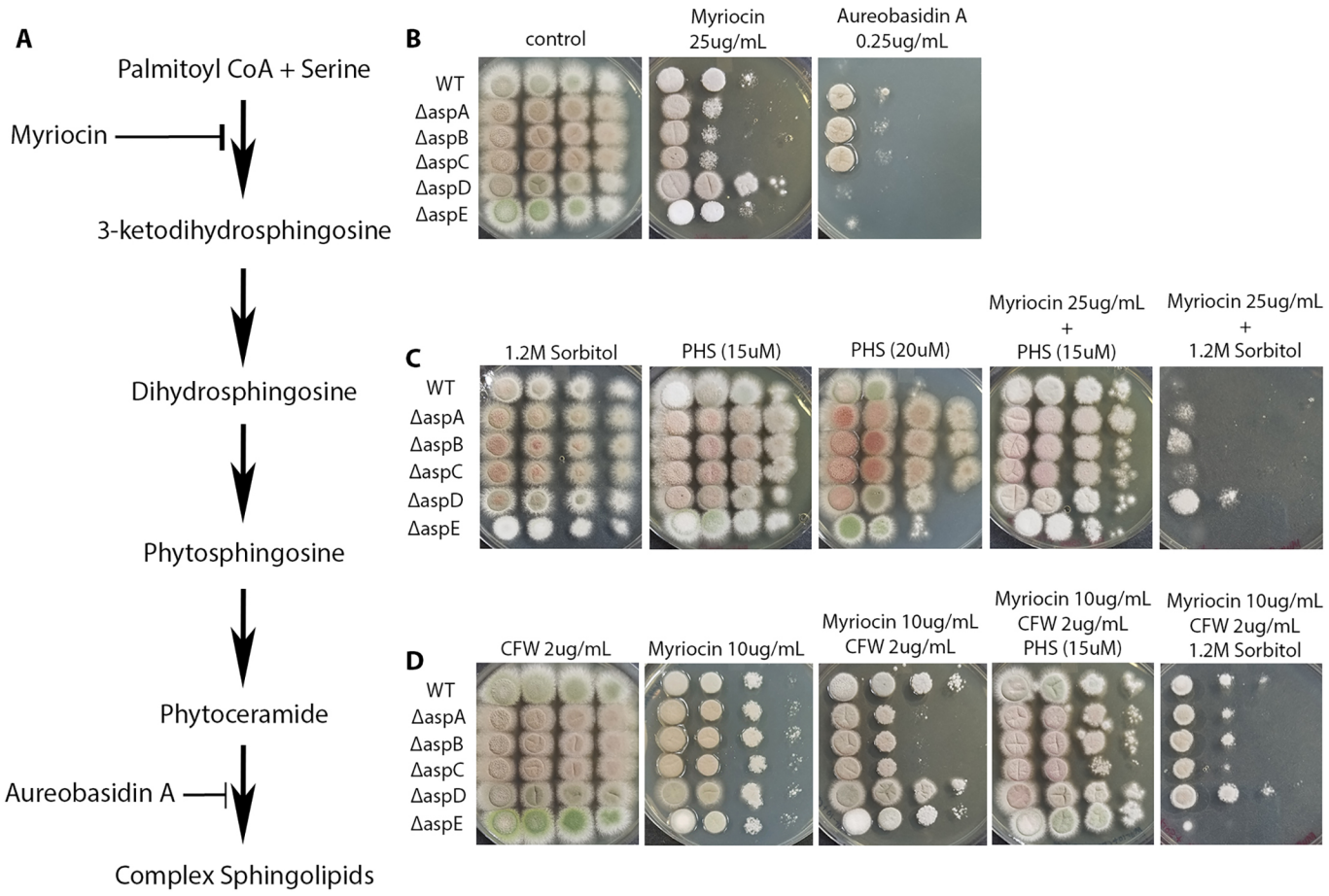


**Fig. 6. Septin core hexamer null mutants show altered sensitivity to agents which disrupt sphingolipid biosynthesis.** (A) A simplified diagram of the sphingolipid biosynthesis pathway in *A. nidulans* (Li et al., 2007). (B) Solid medium spotting assay. WT and septin-null mutants Δ*aspA*$^{cdc11}$, Δ*aspB*$^{cdc3}$, Δ*aspC*$^{cdc12}$, Δ*aspD*$^{cdc10}$ and Δ*aspE* were tested for sensitivity by spotting decreasing spore concentrations on solid medium with or without the sphingolipid biosynthesis-disturbing agents myriocin and aureobasidin A. (C) Rescue of sensitivity to sphingolipid biosynthesis-disturbing agents. WT and septin-null mutants were tested for rescue of sensitivity to sphingolipid biosynthesis-disturbing agents by spotting decreasing spore concentrations on solid medium supplemented with exogenous phytosphingosine (PHS) intermediate (15 µM) or 1.2 M sorbitol, with or without myriocin. (D) Combinatory treatment with cell wall and sphingolipid biosynthesis-disturbing agents. WT and septin-null mutants were tested for sensitivity to cell wall and sphingolipid biosynthesis-disturbing agents in combination, by spotting decreasing spore concentrations on solid medium with or without 'sub-lethal' concentrations of Calcofluor White (CFW), myriocin, or CFW plus myriocin, supplemented with either exogenous phytosphingosine intermediate (15 µM) or 1.2 M sorbitol. Differences in colony color result from changes in spore production, spore pigment and production of secondary metabolites under stress. Spore concentrations were between $10^7$ conidia/ml and $10^4$ conidia/ml for all assays in the figure. The experiment was repeated three times with similar results.

septins may signal sphingolipid status to the CWI pathway, and that this signal is required for proper CWI function.

### Localization of core hexamer septins AspA$^{Cdc11}$ and AspB$^{Cdc3}$ is disrupted by sphingolipid inhibitors

We predicted that, since core septin hexamer null mutants ΔaspA$^{cdc11}$, ΔaspB$^{cdc3}$ and ΔaspC$^{cdc12}$ were sensitive to drugs that inhibit sphingolipid biosynthesis, the localization of these septins might be altered when exposed to the same treatments. We examined whether disruption of sphingolipid biosynthesis causes changes in septin localization using live-cell imaging with fluorescence microscopy. A strain carrying AspA$^{Cdc11}$–GFP was grown in liquid complete medium overnight, treated with exogenous PHS (15 µM) and imaged for 3 h post-treatment. There was a dynamic shift in septin localization under PHS treatment over the course of the experiment, compared to the vehicle control. The septin–GFP signal shifted from a relatively homogenous cortical localization along the hyphal tips to a more stochastic, punctate localization along the entire length of hyphae (Fig. 7, middle panels).

In contrast to these results, treatments with the ergosterol-binding polyene filipin III (25 µg/ml) and the phosphatidylinositol 3-kinase inhibitor wortmannin (20 µg/ml), did not affect the localization pattern of septins as dramatically as the PHS treatment (Fig. 7, left- and right-most panels). Similar patterns of aberrant localization were observed under PHS treatments for AspB$^{Cdc3}$–GFP (Fig. S5). Myriocin treatment also resulted in a similar pattern of mislocalization in AspA$^{Cdc11}$–GFP cells when compared to treatment with PHS (Fig. S6). These results suggest sphingolipid content and/or distribution within the plasma membrane contributes to the localization and stability of core hexamer septins at the plasma membrane and that ergosterol and phosphoinositides may not be as vital for this process.

## DISCUSSION

Our data show that *A. nidulans* septins play roles in both plasma membrane and CWI, and that distinct subgroups of septins carry out these roles. Previous work has shown that the five septins of *A. nidulans* septins form hexamers (AspA$^{Cdc11}$, AspB$^{Cdc3}$ and

Journal of Cell Science (2022) 135, jcs258336. doi:10.1242/jcs.258336

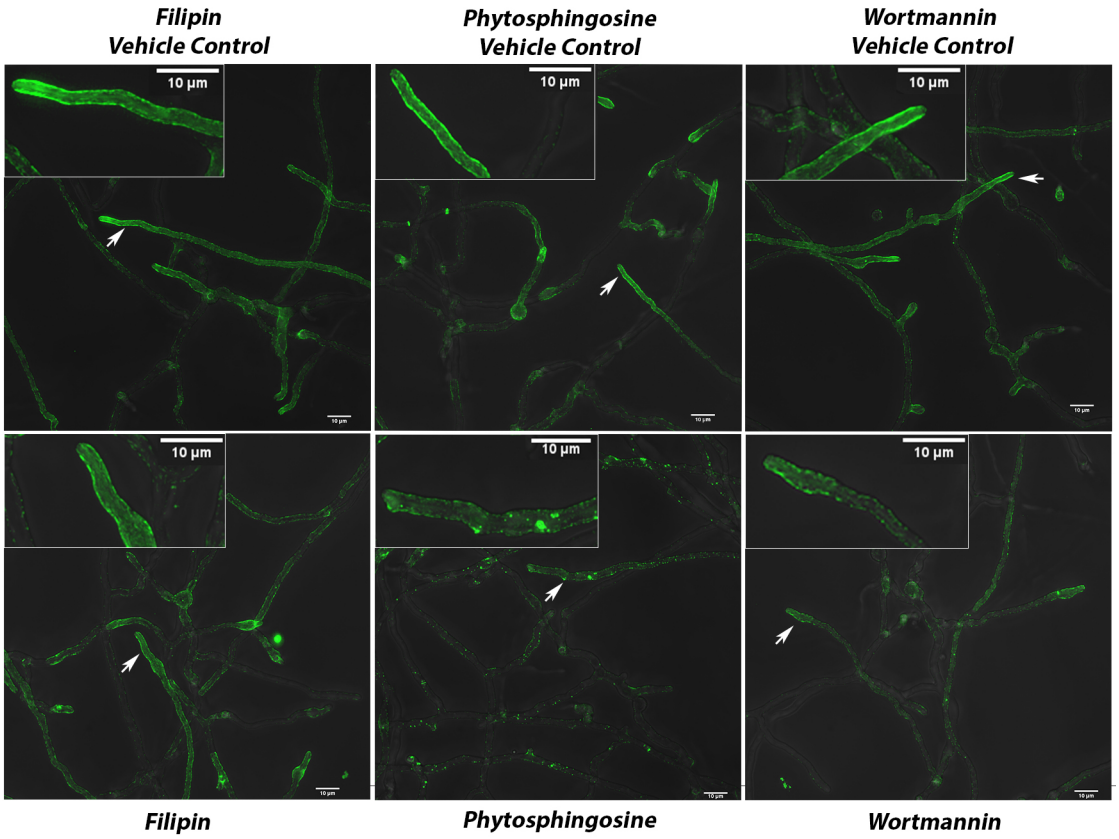


**Fig. 7. Septin AspA$^{Cdc11}$–GFP localization is disrupted by sphingolipid biosynthesis inhibitors.** AspA$^{Cdc11}$–GFP strain incubated in liquid medium for ~16 h and imaged 180 min after replacing with fresh medium containing sterol, sphingolipid and the phosphoinositide-disturbing agents filipin, phytosphingosine and wortmannin, respectively. Representative images are shown from three independent biological replicates with ≥100 cells observed. Top row, vehicle controls for each treatment. Bottom row, filipin (25 µg/ml), phytosphingosine (15 µM) and wortmannin (20 µg/ml) treatments, respectively. Insets show an enlarged section of micrographs from each picture to better visualize pattern of fluorescence signal. Imaging conducted with Deltavision I deconvolution inverted fluorescence microscope. White arrows denote hyphae which are highlighted in enlarged images. Scale bars: 10 µm. The experiment was repeated three times with similar results.

AspC$^{Cdc12}$) and octamers (AspA$^{Cdc11}$, AspB$^{Cdc3}$, AspC$^{Cdc12}$ and AspD$^{Cdc10}$) and that the noncore septin AspE does not appear to be a stable member of a heteropolymer (Hernandez-Rodriguez et al., 2014). The current work suggests that although all septins are involved in coordinating cell wall and membrane integrity, the roles of hexamers, octamers and the noncore septin are somewhat different. Core hexamer septins appear to be most important for sphingolipid metabolism, all five septins appear to be involved in ergosterol metabolism, and core septins are most important for the CWI pathway with the noncore septin possibly playing a minor role. As summarized in Fig. 8 and discussed in more detail below, our previous and current data are consistent with a model in which (1) all five septins assemble at sites of membrane and cell wall remodeling in a sphingolipid-dependent process; (2) all five septins recruit and/or scaffold ergosterol and the core hexamer septins recruit and/or scaffold sphingolipids and associated sensors at these sites, triggering changes in lipid metabolism; and (3) the core septins recruit and/or scaffold CWI machinery to the proper locations and trigger changes in cell wall synthesis. The noncore septin might play a minor role in this process.

### Septins assemble at sites of membrane and cell wall remodeling in a sphingolipid-dependent process

We hypothesize that SRD-associated lipids (ergosterol, sphingolipids and phosphoinositides) recruit or facilitate binding and assembly of septins on the membrane, with sphingolipids contributing more to the stabilization of septins than other SRD-associated lipids in *A. nidulans* (Fig. 8A). Previous studies showed preferential *in vitro* binding of yeast core septin orthologs to the phosphoinositides PIP2, PI(4,5)P2, PI(5)P and PI(4)P; however, our treatments with wortmannin and filipin III, known disruptors of phosphoinositides and ergosterol respectively (de Kruijff and Demel, 1974; Santos et al., 1998; Takeo, 1985; Walker et al., 2000; Wymann et al., 1996), did not affect septin localization as dramatically as sphingolipid-disturbing treatments (Fig. 7; Figs S3 and S4). The marked septin mislocalization we observed upon treatment with PHS and myriocin strongly supports the idea that sphingolipids at the membrane contribute to core septin localization and help maintain septin assemblies at the proper locations. Previous studies on composition of lipid microdomains showed that relatively minor differences in sphingolipid structure can have significant effects on sterol and phospholipid interactions, consequently resulting in major changes in membrane properties (Björkbom et al., 2010; Ramstedt and Slotte, 2006). Perhaps sphingolipids (and ergosterol to a lesser extent) help to stabilize SRDs in a way that facilitates assembly of septin filaments and higher order structures via diffusion, collision and annealing, as proposed by Bridges and colleagues (Bertin et al., 2010; Bridges et al., 2014; Krokowski et al., 2018; Tanaka-Takiguchi et al., 2009). Consistent with this idea, *A. nidulans* AspB filaments have been shown to move along the plasma membrane, break apart and 'snap' together in a

Journal of Cell Science (2022) 135, jcs258336. doi:10.1242/jcs.258336

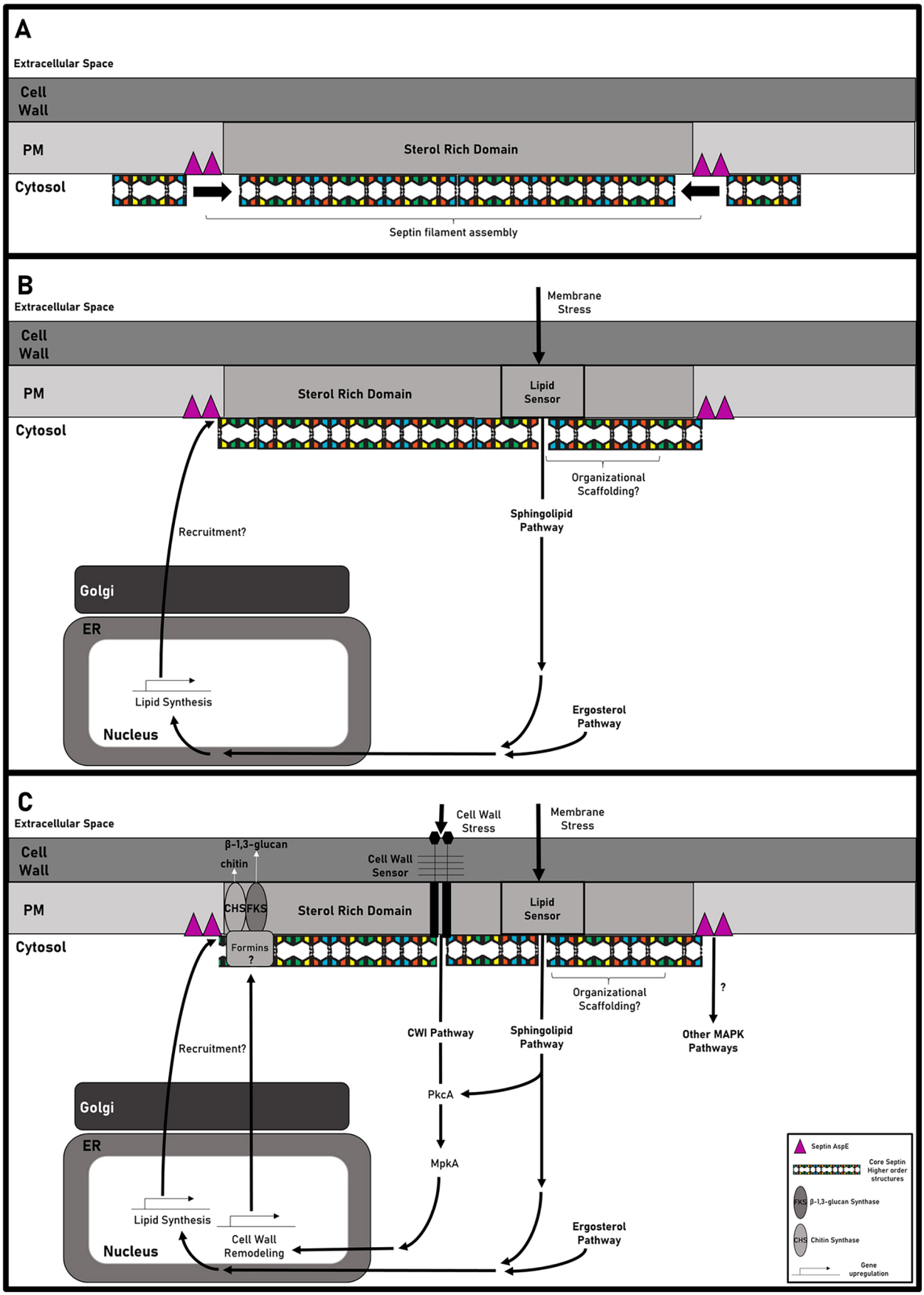


**Fig. 8.** See next page for legend.

**Fig. 8. Model for septin modulation of cell wall and plasma membrane integrity through interactions with SRDs.** As described in the text, our data suggest that all five septins are involved in cell wall and membrane integrity coordination. The core septins that participate in hexamers appear to be most important for sphingolipid metabolism while all septins appear to be involved in ergosterol metabolism and CIW. Because SRDs contain both sphingolipids and ergosterol and because it is not yet clear how subgroups of septins interact with each other at SRDs, we show all core septins in our model without distinguishing hexamers and octamers. In this model, septins are proposed to colocalize with SRDs in a manner that promotes (A) assembly of septins into higher-order structures along the membrane at sites of polarized growth or cell wall/PM remodeling and (B) the recruitment and/or scaffolding of lipids and associated membrane-bound sensors to monitor membrane composition and/or stress. The status of membrane composition is relayed to the nucleus where it triggers changes in expression of genes responsible for lipid metabolism, and (C) the recruitment and/or scaffolding of CWI pathway machinery to monitor cell wall composition and stress, followed by the recruitment and/or scaffolding of cell wall synthases, possibly with the help of other septin-interacting proteins such as formins. Question marks (?) denote speculative processes or interactions that have not been characterized.

way that suggests collision and annealing (Hernandez-Rodriguez et al., 2012).

### Septins recruit and/or scaffold lipids and associated sensors, triggering changes in lipid metabolism

Consistent with a role for septins in modulating membrane composition, all septin-null mutants were resistant to ergosterol-disrupting treatments and core hexamer septin mutants were affected by disruption of sphingolipid biosynthesis (Fig. 5A,B; Fig. 6). Based on proposed mechanisms for septins as diffusion barriers or organizational scaffolds of membrane-associated proteins in yeast and smut fungi, we propose septins monitor lipid microdomain composition and/or organization in filamentous ascomycetes (Canovas and Perez-Martin, 2009; Sugiyama and Tanaka, 2019) (Fig. 8B). Septins do not have a transmembrane domain, a feature that often defines established membrane 'sensors' that monitor local lipid environments (Cho et al., 2019; Nyholm et al., 2007); however, septins share a highly conserved polybasic domain proposed to facilitate septin–membrane interactions (Valadares et al., 2017; Zhang et al., 1999). In addition to the polybasic domain, septins have recently been shown to contain an amphipathic helix motif, which has been implicated in septin sensing of membrane curvatures (Cannon et al., 2019). Given that septins have been shown to assemble into non-polar higher-order structures along the plasma membrane (Bridges et al., 2014), septin assembly itself might be the mechanism by which lipid composition and protein organization is monitored at the cytosolic face of membranes. Perhaps septin assemblies that pass specific size or geometric thresholds trigger signaling through MAPK and other pathways.

### Core septins recruit and/or scaffold CWI machinery to the proper locations and trigger changes in cell wall synthesis

In addition to monitoring and relaying information about the membrane, septins clearly have a role in normal cell wall growth and remediation of cell wall stress via the CWI pathway. We propose a major role of the core septins is to recruit and/or organize integral proteins to sites of polarized growth or remodeling at the cell cortex to ensure CWI pathway functions are carried out (Fig. 8C). The sensitivity to cell wall-disturbing agents, altered cell wall composition and altered polysaccharide deposition in the core septin-null mutants (Figs 1,2; Figs S1,S2) are consistent with phenotypes of CWI pathway mutants in previous studies (Valiante et al., 2008, 2009, 2015). Our glycosyl linkage analysis showed that cell wall chitin content is increased in the septin mutant cells compared to WT cells (Fig. S2). Hyper-synthesis of chitin has been shown to occur during cell wall stress via the CWI pathway in *S. cerevisiae* and *Candida albicans* (Dallies et al., 1998; Kapteyn et al., 2000, 1997; Lagorce et al., 2002; Osmond et al., 1999; Popolo et al., 1997; Ram et al., 1998, 1994). Double mutant analyses between septins and CWI pathway kinases also support a role for core septins in maintaining CWI under stress (Fig. 4). Suppression of cell wall defects under cell wall stress by deletion of septins in an $\Delta mpkA^{slt2}$ background suggests that a parallel node by which septins negatively regulate CWI pathway sensors or kinases could exist. This interpretation is consistent with studies in yeast showing that Bni4 (ANID_00979), a formin which is phosphorylated by and functions downstream of MAPK $Slt2^{mpkA}$, directly interacts with the core septin orthologs in order to recruit chitin synthases to the bud neck (Heinisch and Rodicio, 2018; Larson et al., 2010; Perez et al., 2016). Although the involvement of AspE in the CWI pathway appears to be minor based on the very mild sensitivity of the null mutant to Congo Red (Fig. 1), sensitivity to TOR and cAMP-PKA pathway inhibitors suggests that AspE might participate indirectly through MAPK pathway crosstalk (Fig. S4). It could be that, in the septin-null mutants, septin filaments are not able to properly assemble and monitor lipid composition and protein organization at the cytosolic face of membranes, resulting in defects in plasma membrane and CWI (Fig. 8).

Although we have discussed membrane and CWI separately, it is possible that membrane defects in the septin-null mutants contribute to the observed cell wall changes or that cell wall defects contribute to the observed changes in lipid metabolism. When septin deletion mutants were challenged with both membrane-disturbing and cell wall-disturbing agents in combination, rescue of the lipid defect (via PHS) restored proper growth, but rescue of the cell wall defect (via sorbitol) did not rescue lethality (Fig. 6C,D). This suggests that there is a synergistic effect of disrupting sphingolipid metabolism and cell wall architecture in septin-null mutants and that septin–sphingolipid interactions are required for roles in maintaining CWI.

Because *A. nidulans* septin deletion mutants are viable, we were able to systematically analyze the roles of all septins in this organism. Our data show that all septins are required for proper coordination of lipid metabolism, with core hexamer septins most important for sphingolipid metabolism and all septins involved in ergosterol metabolism. Our data also show that the core septins are most important for the CWI pathway, but that these roles require sphingolipids. Based on our data, we propose that septins are critical for tight coordination of plasma membrane metabolism and cell wall synthesis during normal development and response to exogenous stress, and that the site of this coordination is likely SRDs. Future work will address how subgroups of septins interact with each other and with sphingolipids and ergosterol in SRDs to coordinate the CWI response.

## MATERIALS AND METHODS

### Spore dilution drug sensitivity assays

Strains used in this study are listed in Table S1. Media used were previously described (Harris et al., 1994). *Aspergillus nidulans* strains were harvested in double-distilled water ($ddH_2O$), spores normalized to $10^7$ or $10^6$ conidia/ml, and then serial diluted 4-fold into separate Eppendorf tubes. All strains were inoculated in 10 µl droplets in a grid pattern on Petri plates containing 25 ml of solid (1.8% agar) complete medium (CM) (1% glucose, 0.2% peptone, 0.1% casamino acids, 0.1% yeast extract, trace elements, nitrate salts and 0.01% vitamins, pH 6.5; with amino acid supplements as noted) or minimal medium (MM) (1% glucose, trace elements, 1% thiamine, 0.05% biotin, pH 6.5; with amino acid supplements as noted) with or without

amended supplements. All incubations were conducted at 30°C as indicated for 3–4 days before images were taken. Sorbitol, NaCl and KCl were added at 2 M, 1 M and 1.5 M, respectively, to media before autoclaving. Stock solutions were prepared as follows: Blankophor BBH/CFW (Bayer Corporation; standard-SV-2460; 25 mg/ml in $ddH_2O$ and adjusted pH with 1 M KOH until solubilized), Congo Red (Fisher Scientific; Lot No.8232-6; 10 mg/ml in $ddH_2O$), caspofungin acetate (1 mg/ml in $ddH_2O$), fludioxonil/pestanal (2 mg/ml in DMSO) and caffeine monohydrate (63.66 mg/ml in $ddH_2O$ and gently heated with stirring until solubilized); calcium chloride (2 M in $ddH_2O$), EGTA (0.5 M in $ddH_2O$), rapamycin/sirolimus (1 mg/ml in acetonitrile), FK-506 (5 mg/ml in DMSO), natamycin (1.5 mg/ml in MeOH), itraconazole (10 mg/ml in DMSO), terbinafine (10 mg/ml in DMSO). Stock solutions of myriocin (5 mg/ml), phytosphingosine (1 mg/ml) and aureobasidin A (1 mg/ml) were prepared in DMSO, ethanol and methanol, respectively and stored at −20°C in the dark. Images of plates were captured using a cellular device with an 8.0 Megapixel camera, and subsequently processed using Photoshop CS5 Version 12.0 X32.

### Generating double mutants and other strains by crossing

Parental strains were co-inoculated in CM liquid at $10^5$ conidia/ml supplemented with all parental auxotrophic markers and allowed to incubate at 30°C for up to 1 week or until a thick mycelial mat had formed. Mycelial mats were transferred to solid MM plates containing only shared auxotrophic markers from the genetic backgrounds of each parental strain. Plates containing mycelial mats were covered with parafilm and incubated in the dark at room temperature for up to 2 weeks or until mature cleistothecia formed on the mycelial mats. Multiple cleistothecia from each genetic cross were collected in water, diluted and plated onto solid medium containing all auxotrophic supplements from each parental strain to allow growth of all resulting progeny. Approximately 50 progenies were collected from each dissected cleistothecium, and each colony was transferred to master plates and replica-plated onto MM without any supplements, to isolate prototrophic progeny. Five to ten progenies from each cross were then 3-phased streaked to obtain single colony isolates for PCR verification. All progenies of genetic crosses were verified by diagnostic PCR using KOD XTREME Hot Start DNA Polymerase (71975-3, EMD Millipore) or OneTaq® Hot Start Quick-Load® 2X Master Mix with Standard Buffer (M0488L, New England BioLabs Inc.) according to the manufacturer's instructions. Double mutant strains of $\Delta mpkA^{slt2}$ were verified for deletion of $mpkA^{slt2}$ by amplification of entire gene using primers, MpkA-806-F' and MpkA-3779-R', followed by SacI HF restriction enzyme digestion of PCR product to better visualize band sizes. All progeny from chitin synthase and septin-null mutant crosses were determined to be virtually identical to each septin mutant parental strain in growth/morphology on a colony level and by microscopy, PCR-verified for the deletion of each septin gene, and screened visually by fluorescence microscopy for the presence of chitin synthase–GFP signal. Chitin synthase–GFP strains in a $\Delta aspA^{cdc11}$ genetic background were verified for deletion of $aspA^{cdc11}$ by amplification of the entire gene using primers, AspA-KO-F' and AspA-KO-R', followed by XhoI restriction enzyme digestion for verification of band sizes. Strains and primer sets used in this study can be found in Tables S1 and S2, respectively.

### Growth conditions and microscopy

Growth and preparation of cells were as previously reported (Momany et al., 1999). Conidia were inoculated on sterile coverslips in 10 ml liquid complete medium or MM at $10^5$ conidia/ml and incubated at 30°C in a small Petri dish for the specified amount of time. Cell walls were stained for chitin with Blankophor BBH (CFW) (American Cyanamid, Wayne, NJ; 25 mg/ml stock solution in $ddH_2O$ and pH adjusted by 1 M KOH until solubilized; working solution made by diluting stock solution by 100× and 8 µl dissolved in 5 ml $ddH_2O$ prepared fresh for working solution and used immediately), β-(1,3)-glucans were stained with Aniline Blue (stock solution prepared fresh to 10 mg/ml final concentration in $ddH_2O$; working solution prepared at 135.55 µM in 50 mM phosphate buffer, pH adjusted to 9.5 with 5 M KOH, and used immediately; coverslips stained for 5 min in the dark at room temperature). Live-cell imaging experiments tracking septin localization were conducted using filipin III (stock solution prepared at 5 mg/ml in DMSO; working solution was used at 25 µg/ml final concentration in liquid complete medium), phytosphingosine (working solution was used at 15 µM in liquid complete medium) and wortmannin (stock solution prepared to 2 mg/ml in DMSO; working solution was used at 20 µg/ml in liquid complete medium). Vehicle controls and conducted at ≤1% (w/v) in liquid medium. Imaging was performed in the Biomedical Microscopy Core at the University of Georgia.

Microscopy was carried out using Zeiss Axioplan microscope and Zeiss Axiocam MRc charge-coupled device camera and software, as well as a Deltavision I deconvolution inverted microscope and LSM880 confocal fluorescent microscope with diode laser (405 nm), argon (458, 488, 514 nm) and HeNe (543, 633 nm) laser lines. All micrograph comparisons between treatments imaged with identical microscope settings. Subsequent image analysis and scale bars added to micrographs, using ImageJ software 1.48v, Java 1.6.0_20 (64-bit) or Zen 2.3 imaging software, and final figures compiled in Photoshop CS5 software version 12.0 ×32.

### Quantification of Aniline Blue and CFW staining patterns by line scans

Maximum projection images were made and scale bars added for each micrograph in Zen (Black) Edition. Micrographs were false colored black and white, line scans were drawn by hand through hyphal tips, line scan profiles were generated in Zen 3.1 (Blue) imaging software, and associated data points for each profile were exported to Microsoft Excel version 2004 (Build 12730.20270) to create graphs and conduct statistical analysis. Figures were generated using Adobe Photoshop 2020 Version 21.1.2.

### Quantification of chitin synthase–GFP and CFW fluorescence signal by line scans

Maximum projection images were made for each micrograph, line scans were drawn by hand through hyphal branch tips in ImageJ software 1.48v, and data points were exported to Microsoft Excel version 2004 (Build 12730.20270) to create graphs and conduct statistical analysis. Figures were assembled using Adobe Photoshop 2020 Version: 21.1.2.

### Cell wall extraction

Cell walls were isolated from a protocol based on Bull (1970); cell wall extraction and lyophilization were conducted as previously described in Guest and Momany (2000) with slight modifications listed in full procedure here. A single batch of complete medium (as described above) was autoclaved and supplements added: arginine, methionine, pyridoxine and riboflavin, were added to single flask and then distributed to individual flasks to be inoculated. $10^4$ conidia/ml were inoculated in two flasks each of 100 ml liquid complete medium. Flasks were incubated at 30°C in orbital shaker at 200 rpm for 48 h. Mycelia was gravity filtrated, then vacuum-filtrated through #42 Whatman filter paper, subsequently washed with 50 ml each of chilled $ddH_2O$ to remove residual medium and stored at −80°C until completely frozen. Mycelium from each sample was allowed to thaw on ice and then washed sequentially with 50 ml chilled $ddH_2O$ and 0.5 M NaCl. Fungal hyphal mats were transferred to mortar and pestle, then subsequently flash frozen in liquid nitrogen and ground in chilled Tris/EDTA disruption buffer (DB; 20 mM Tris-HCl pH 8.0, 50 mM EDTA) with a pre-chilled mortar and pestle. Samples were monitored by microscopy under a 60× or 100× objective until hyphal ghosts were evident. Cell walls were separated by centrifugation at 13,800 ***g*** for 10 min at 4°C. The cell pellet was placed in a beaker with 40–100 ml of chilled Tris/EDTA buffer and stirred at 4°C for 12 h. The cell pellet was collected by centrifugation as above and stirred again with 100 ml chilled $ddH_2O$ at 4°C for 4 h. Cell wall material was collected by vacuum filtration, frozen at −80°C, lyophilized until dry and stored at room temperature (25°C) for further analysis.

### Cell wall glycosyl linkage analysis

To determine the glycosyl linkages, the samples were acetylated using pyridine and acetic anhydride in order to get better solubility, before two rounds of permethylation using sodium hydroxide (15 min) and methyl iodide (45 min). The permethylated material was hydrolyzed using 2 M trifluoroacetic acid (TFA; 2 h in sealed tube at 121°C), reduced with $NaBD_4$ and acetylated using acetic anhydride/pyridine. The resulting partially methylated alditol acetates (PMAAs; neutral sugars) were analyzed on an Agilent 7890A GC interfaced to

a 5975C MSD (mass selective detector, electron impact ionization mode); separation was performed on a 30 m Supelco SP-2331 bonded phase fused silica capillary column using Supelco SP-2331 fused silica capillary column [30 m×0.25 mm internal diameter (ID)]. The PMAAs of amino sugars were separated on Supelco Equity-1 column (30 m×0.25 mm ID). Furthermore, the relative quantities of respective glycosyl linkages were calculated by integrating the peak area of respective peak. Since the neutral and amino sugars were analyzed on different instruments, the peak area of amino sugars was normalized to the value for the 4-Glc peak, which is prominent in both the instruments and the integrated and normalized peak areas were pooled together to calculate the relative percentage of individual linkages. Two independent, biological replicates were conducted for this analysis and processed in tandem. The average area (%) of detected linkages of one representative data set is included in the graphs to show relative differences between cell wall polysaccharides between samples.

#### Acknowledgements
Chitin synthase strains were generously provided by Dr Hiroyuki Horiuchi in the Department of Biotechnology at the University of Tokyo.

#### Competing interests
The authors declare no competing or financial interests.

#### Author contributions
Conceptualization: A.M., M.M.; Methodology: A.M., M.M.; Formal analysis: A.M., M.M.; Investigation: A.M.; Writing - original draft: A.M., M.M.; Writing - review & editing: A.M., M.M.; Visualization: A.M.; Supervision: M.M.; Funding acquisition: M.M.

#### Funding
These studies were supported by the University of Georgia and Franklin College of Arts & Sciences support to M.M. and Plant Biology Department support to A.M. The glycosyl linkage analysis was supported by a Chemical Sciences, Geosciences and Biosciences Division, Office of Basic Energy Sciences, U.S. Department of Energy grant (DE-SC0015662) to Parastoo Azadi at the Complex Carbohydrate Research Center at UGA.

#### Peer review history
The peer review history is available online at
https://journals.biologists.com/jcs/article-lookup/DOI/10.1242/jcs.258336

#### References
**Alvarez, F. J., Douglas, L. M. and Konopka, J. B.** (2007). Sterol-rich plasma membrane domains in fungi. *Eukaryot. Cell* **6**, 755-763. doi:10.1128/EC.00008-07

**Badrane, H., Nguyen, M. H. and Clancy, C. J.** (2016). Highly dynamic and specific phosphatidylinositol 4,5-bisphosphate, septin, and cell wall integrity pathway responses correlate with caspofungin activity against candida albicans. *Antimicrob. Agents Chemother.* **60**, 3591-3600. doi:10.1128/AAC.02711-15

**Bagnat, M. and Simons, K.** (2002). Lipid rafts in protein sorting and cell polarity in budding yeast Saccharomyces cerevisiae. *Biol. Chem.* **383**, 1475-1480. doi:10.1515/BC.2002.169

**Barbet, N. C., Schneider, U., Helliwell, S. B., Stansfield, I., Tuite, M. F. and Hall, M. N.** (1996). TOR controls translation initiation and early G1 progression in yeast. *Mol. Biol. Cell* **7**, 25-42. doi:10.1091/mbc.7.1.25

**Beh, C. T., Alfaro, G., Duamel, G., Sullivan, D. P., Kersting, M. C., Dighe, S., Kozminski, K. G. and Menon, A. K.** (2009). Yeast oxysterol-binding proteins: sterol transporters or regulators of cell polarization? *Mol. Cell. Biochem.* **326**, 9-13. doi:10.1007/s11010-008-9999-7

**Bertin, A., McMurray, M. A., Grob, P., Park, S.-S., Garcia, G., III, Patanwala, I., Ng, H.-L., Alber, T., Thorner, J. and Nogales, E.** (2008). Saccharomyces cerevisiae septins: supramolecular organization of heterooligomers and the mechanism of filament assembly. *Proc. Natl. Acad. Sci. USA* **105**, 8274-8279. doi:10.1073/pnas.0803330105

**Bertin, A., McMurray, M. A., Thai, L., Garcia, G., III, Votin, V., Grob, P., Allyn, T., Thorner, J. and Nogales, E.** (2010). Phosphatidylinositol-4,5-bisphosphate promotes budding yeast septin filament assembly and organization. *J. Mol. Biol.* **404**, 711-731. doi:10.1016/j.jmb.2010.10.002

**Binder, U., Oberparleiter, C., Meyer, V. and Marx, F.** (2010). The antifungal protein PAF interferes with PKC/MPK and cAMP/PKA signalling of Aspergillus nidulans. *Mol. Microbiol.* **75**, 294-307. doi:10.1111/j.1365-2958.2009.06936.x

**Björkbom, A., Róg, T., Kaszuba, K., Kurita, M., Yamaguchi, S., Lönnfors, M., Nyholm, T. K. M., Vattulainen, I., Katsumura, S. and Slotte, J. P.** (2010). Effect of sphingomyelin headgroup size on molecular properties and interactions with cholesterol. *Biophys. J.* **99**, 3300-3308. doi:10.1016/j.bpj.2010.09.049

**Blankenship, J. R., Fanning, S., Hamaker, J. J. and Mitchell, A. P.** (2010). An extensive circuitry for cell wall regulation in Candida albicans. *PLoS Pathog.* **6**, e1000752. doi:10.1371/journal.ppat.1000752

**Bridges, A. A. and Gladfelter, A. S.** (2015). Septin form and function at the cell cortex. *J. Biol. Chem.* **290**, 17173-17180. doi:10.1074/jbc.R114.634444

**Bridges, A. A., Zhang, H., Mehta, S. B., Occhipinti, P., Tani, T. and Gladfelter, A. S.** (2014). Septin assemblies form by diffusion-driven annealing on membranes. *Proc. Natl. Acad. Sci. USA* **111**, 2146-2151. doi:10.1073/pnas.1314138111

**Bulawa, C. E., Miller, D. W., Henry, L. K. and Becker, J. M.** (1995). Attenuated virulence of chitin-deficient mutants of Candida albicans. *Proc. Natl. Acad. Sci. USA* **92**, 10570-10574. doi:10.1073/pnas.92.23.10570

**Butcher, F. R. and Potter, V. R.** (1972). Control of the adenosine 3',5'-monophosphate-adenyl cyclase system in the livers of developing rats. *Cancer Res.* **32**, 2141-2147.

**Bull, A. T.** (1970). Chemical composition of wild-type and mutant Aspergillus nidulans cell walls. The nature of polysaccharide and melanin constituents. J. Gen. *Microbiol.* **63**, 75-94. doi:10.1099/00221287-63-1-75.

**Cannon, K. S., Woods, B. L., Crutchley, J. M. and Gladfelter, A. S.** (2019). An amphipathic helix enables septins to sense micrometer-scale membrane curvature. *J. Cell Biol.* **218**, 1128-1137. doi:10.1083/jcb.201807211

**Canovas, D. and Perez-Martin, J.** (2009). Sphingolipid biosynthesis is required for polar growth in the dimorphic phytopathogen Ustilago maydis. *Fungal Genet. Biol.* **46**, 190-200. doi:10.1016/j.fgb.2008.11.003

**Cardenas, M. E., Cutler, N. S., Lorenz, M. C., Di Como, C. J. and Heitman, J.** (1999). The TOR signaling cascade regulates gene expression in response to nutrients. *Genes Dev.* **13**, 3271-3279. doi:10.1101/gad.13.24.3271

**Caudron, F. and Barral, Y.** (2009). Septins and the lateral compartmentalization of eukaryotic membranes. *Dev. Cell* **16**, 493-506. doi:10.1016/j.devcel.2009.04.003

**Cheng, J., Park, T.-S., Fischl, A. S. and Ye, X. S.** (2001). Cell cycle progression and cell polarity require sphingolipid biosynthesis in Aspergillus nidulans. *Mol. Cell. Biol.* **21**, 6198-6209. doi:10.1128/MCB.21.18.6198-6209.2001

**Cho, H., Stanzione, F., Oak, A., Kim, G. H., Yerneni, S., Qi, L., Sum, A. K. and Chan, C.** (2019). Intrinsic structural features of the human IRE1alpha transmembrane domain sense membrane lipid saturation. *Cell Rep* **27**, 307-320.e5. doi:10.1016/j.celrep.2019.03.017

**Clay, L., Caudron, F., Denoth-Lippuner, A., Boettcher, B., Buvelot Frei, S., Snapp, E. L. and Barral, Y.** (2014). A sphingolipid-dependent diffusion barrier confines ER stress to the yeast mother cell. *Elife* **3**, e01883. doi:10.7554/eLife.01883

**Colabardini, A. C., Ries, L. N., Brown, N. A., Savoldi, M., Dinamarco, T. M., von Zeska Kress, M. R., Goldman, M. H. and Goldman, G. H.** (2014). Protein kinase C overexpression suppresses calcineurin-associated defects in Aspergillus nidulans and is involved in mitochondrial function. *PLoS ONE* **9**, e104792. doi:10.1371/journal.pone.0104792

**Costanzo, M., Baryshnikova, A., Bellay, J., Kim, Y., Spear, E. D., Sevier, C. S., Ding, H., Koh, J. L., Toufighi, K., Mostafavi, S. et al.** (2010). The genetic landscape of a cell. *Science* **327**, 425-431. doi:10.1126/science.1180823

**Dallies, N., Francois, J. and Paquet, V.** (1998). A new method for quantitative determination of polysaccharides in the yeast cell wall. Application to the cell wall defective mutants of Saccharomyces cerevisiae. *Yeast* **14**, 1297-1306. doi:10.1002/(SICI)1097-0061(1998100)14:14<1297::AID-YEA310>3.0.CO;2-L

**de Almeida, R. F. M.** (2018). A route to understanding yeast cellular envelope - plasma membrane lipids interplaying in cell wall integrity. *FEBS J.* **285**, 2402-2404. doi:10.1111/febs.14526

**de Kruijff, B. and Demel, R. A.** (1974). Polyene antibiotic-sterol interactions in membranes of Acholeplasma laidlawii cells and lecithin liposomes. 3. Molecular structure of the polyene antibiotic-cholesterol complexes. *Biochim. Biophys. Acta* **339**, 57-70. doi:10.1016/0005-2736(74)90332-0

**Dickson, R. C.** (2008). Thematic review series: sphingolipids. New insights into sphingolipid metabolism and function in budding yeast. *J. Lipid Res.* **49**, 909-921. doi:10.1194/jlr.R800003-JLR200

**Dobbelaere, J. and Barral, Y.** (2004). Spatial coordination of cytokinetic events by compartmentalization of the cell cortex. *Science* **305**, 393-396. doi:10.1126/science.1099892

**Dongo, A., Bataille-Simoneau, N., Campion, C., Guillemette, T., Hamon, B., Iacomi-Vasilescu, B., Katz, L. and Simoneau, P.** (2009). The group III two-component histidine kinase of filamentous fungi is involved in the fungicidal activity of the bacterial polyketide ambruticin. *Appl. Environ. Microbiol.* **75**, 127-134. doi:10.1128/AEM.00993-08

**Fitzgibbon, G. J., Morozov, I. Y., Jones, M. G. and Caddick, M. X.** (2005). Genetic analysis of the TOR pathway in Aspergillus nidulans. *Eukaryot. Cell* **4**, 1595-1598. doi:10.1128/EC.4.9.1595-1598.2005

**Foderaro, J. E., Douglas, L. M. and Konopka, J. B.** (2017). MCC/eisosomes regulate cell wall synthesis and stress responses in fungi. *J Fungi (Basel)* **3**, 61. doi:10.3390/jof3040061

**Fortwendel, J. R., Juvvadi, P. R., Perfect, B. Z., Rogg, L. E., Perfect, J. R. and Steinbach, W. J.** (2010). Transcriptional regulation of chitin synthases by

calcineurin controls paradoxical growth of Aspergillus fumigatus in response to caspofungin. *Antimicrob. Agents Chemother.* **54**, 1555-1563. doi:10.1128/AAC.00854-09

**Fujioka, A., Terai, K., Itoh, R. E., Aoki, K., Nakamura, T., Kuroda, S., Nishida, E. and Matsuda, M.** (2006). Dynamics of the Ras/ERK MAPK cascade as monitored by fluorescent probes. *J. Biol. Chem.* **281**, 8917-8926. doi:10.1074/jbc.M509344200

**Fukuda, K., Yamada, K., Deoka, K., Yamashita, S., Ohta, A. and Horiuchi, H.** (2009). Class III chitin synthase ChsB of Aspergillus nidulans localizes at the sites of polarized cell wall synthesis and is required for conidial development. *Eukaryot. Cell* **8**, 945-956. doi:10.1128/EC.00326-08

**Garcia-Rodriguez, L. J., Trilla, J. A., Castro, C., Valdivieso, M. H., Duran, A. and Roncero, C.** (2000). Characterization of the chitin biosynthesis process as a compensatory mechanism in the fks1 mutant of Saccharomyces cerevisiae. *FEBS Lett.* **478**, 84-88. doi:10.1016/S0014-5793(00)01835-4

**Garcia, R., Bravo, E., Diez-Muniz, S., Nombela, C., Rodriguez-Pena, J. M. and Arroyo, J.** (2017). A novel connection between the cell wall integrity and the PKA pathways regulates cell wall stress response in yeast. *Sci. Rep.* **7**, 5703. doi:10.1038/s41598-017-06001-9

**Gladfelter, A. S., Pringle, J. R. and Lew, D. J.** (2001). The septin cortex at the yeast mother-bud neck. *Curr. Opin. Microbiol.* **4**, 681-689. doi:10.1016/S1369-5274(01)00269-7

**Glomb, O. and Gronemeyer, T.** (2016). Septin organization and functions in budding yeast. *Front. Cell Dev. Biol.* **4**, 123. doi:10.3389/fcell.2016.00123

**Guest, G. M. and Momany, M.** (2000). Analysis of cell wall sugars in the pathogen Aspergillus fumigatus and the saprophyte Aspergillus nidulans. *Mycologia* **92**, 1047-1050. doi:10.1080/00275514.2000.12061250

**Harris, S. D., Morrell, J. L. and Hamer, J. E.** (1994). Identification and characterization of Aspergillus nidulans mutants defective in cytokinesis. *Genetics* **136**, 517-532. doi:10.1093/genetics/136.2.517

**Harvald, E. B., Olsen, A. S. and Faergeman, N. J.** (2015). Autophagy in the light of sphingolipid metabolism. *Apoptosis* **20**, 658-670. doi:10.1007/s10495-015-1108-2

**Heinisch, J. J. and Rodicio, R.** (2018). Protein kinase C in fungi-more than just cell wall integrity. *FEMS Microbiol. Rev.* **42**, fux051. doi:10.1093/femsre/fux051

**Hernandez-Rodriguez, Y., Hastings, S. and Momany, M.** (2012). The septin AspB in Aspergillus nidulans forms bars and filaments and plays roles in growth emergence and conidiation. *Eukaryot. Cell* **11**, 311-323. doi:10.1128/EC.05164-11

**Hernandez-Rodriguez, Y., Masuo, S., Johnson, D., Orlando, R., Smith, A., Couto-Rodriguez, M. and Momany, M.** (2014). Distinct septin heteropolymers co-exist during multicellular development in the filamentous fungus Aspergillus nidulans. *PLoS ONE* **9**, e92819. doi:10.1371/journal.pone.0092819

**Hohmann, S.** (2002). Osmotic stress signaling and osmoadaptation in yeasts. *Microbiol. Mol. Biol. Rev.* **66**, 300-372. doi:10.1128/MMBR.66.2.300-372.2002

**Kapteyn, J. C., Ram, A. F., Groos, E. M., Kollar, R., Montijn, R. C., Van Den Ende, H., Llobell, A., Cabib, E. and Klis, F. M.** (1997). Altered extent of cross-linking of beta1,6-glucosylated mannoproteins to chitin in Saccharomyces cerevisiae mutants with reduced cell wall beta1,3-glucan content. *J. Bacteriol.* **179**, 6279-6284. doi:10.1128/JB.179.20.6279-6284.1997

**Kapteyn, J. C., Hoyer, L. L., Hecht, J. E., Muller, W. H., Andel, A., Verkleij, A. J., Makarow, M., Van Den Ende, H. and Klis, F. M.** (2000). The cell wall architecture of Candida albicans wild-type cells and cell wall-defective mutants. *Mol. Microbiol.* **35**, 601-611. doi:10.1046/j.1365-2958.2000.01729.x

**Kojima, K., Bahn, Y. S. and Heitman, J.** (2006). Calcineurin, Mpk1 and Hog1 MAPK pathways independently control fludioxonil antifungal sensitivity in Cryptococcus neoformans. *Microbiology* **152**, 591-604. doi:10.1099/mic.0.28571-0

**Kopecka, M. and Gabriel, M.** (1992). The influence of congo red on the cell wall and (1→3)-beta-D-glucan microfibril biogenesis in Saccharomyces cerevisiae. *Arch. Microbiol.* **158**, 115-126. doi:10.1007/BF00245214

**Kovacs, Z., Szarka, M., Kovacs, S., Boczonadi, I., Emri, T., Abe, K., Pocsi, I. and Pusztahelyi, T.** (2013). Effect of cell wall integrity stress and RlmA transcription factor on asexual development and autolysis in Aspergillus nidulans. *Fungal Genet. Biol.* **54**, 1-14. doi:10.1016/j.fgb.2013.02.004

**Krokowski, S., Lobato-Marquez, D., Chastanet, A., Pereira, P. M., Angelis, D., Galea, D., Larrouy-Maumus, G., Henriques, R., Spiliotis, E. T., Carballido-Lopez, R. et al.** (2018). Septins recognize and entrap dividing bacterial cells for delivery to lysosomes. *Cell Host Microbe* **24**, 866-874.e4. doi:10.1016/j.chom.2018.11.005

**Kuranda, K., Leberre, V., Sokol, S., Palamarczyk, G. and Francois, J.** (2006). Investigating the caffeine effects in the yeast Saccharomyces cerevisiae brings new insights into the connection between TOR, PKC and Ras/cAMP signalling pathways. *Mol. Microbiol.* **61**, 1147-1166. doi:10.1111/j.1365-2958.2006.05300.x

**Lagorce, A., Le Berre-Anton, V., Aguilar-Uscanga, B., Martin-Yken, H., Dagkessamanskaia, A. and Francois, J.** (2002). Involvement of GFA1, which encodes glutamine-fructose-6-phosphate amidotransferase, in the activation of the chitin synthesis pathway in response to cell-wall defects in Saccharomyces cerevisiae. *Eur. J. Biochem.* **269**, 1697-1707. doi:10.1046/j.1432-1327.2002.02814.x

**Larson, J. R., Kozubowski, L. and Tatchell, K.** (2010). Changes in Bni4 localization induced by cell stress in Saccharomyces cerevisiae. *J. Cell Sci.* **123**, 1050-1059. doi:10.1242/jcs.066258

**Li, S., Bao, D., Yuen, G., Harris, S. D. and Calvo, A. M.** (2007). basA regulates cell wall organization and asexual/sexual sporulation ratio in Aspergillus nidulans. *Genetics* **176**, 243-253. doi:10.1534/genetics.106.068239

**Longtine, M. S. and Bi, E.** (2003). Regulation of septin organization and function in yeast. *Trends Cell Biol.* **13**, 403-409. doi:10.1016/S0962-8924(03)00151-X

**Manfiolli, A. O., Mattos, E. C., de Assis, L. J., Silva, L. P., Ulas, M., Brown, N. A., Silva-Rocha, R., Bayram, O. and Goldman, G. H.** (2019). Aspergillus fumigatus high osmolarity glycerol mitogen activated protein kinases SakA and MpkC physically interact during osmotic and cell wall stresses. *Front. Microbiol.* **10**, 918. doi:10.3389/fmicb.2019.00918

**Martin, S. W. and Konopka, J. B.** (2004). Lipid raft polarization contributes to hyphal growth in Candida albicans. *Eukaryot. Cell* **3**, 675-684. doi:10.1128/EC.3.3.675-684.2004

**McMurray, M. A. and Thorner, J.** (2019). Turning it inside out: the organization of human septin hetero-oligomers. *Cytoskeleton (Hoboken)* **76**, 449-456. doi:10.1002/cm.21571

**McMurray, M. A., Bertin, A., Garcia, G., III, Lam, L., Nogales, E. and Thorner, J.** (2011). Septin filament formation is essential in budding yeast. *Dev. Cell* **20**, 540-549. doi:10.1016/j.devcel.2011.02.004

**Merlini, L., Bolognesi, A., Juanes, M. A., Vandermoere, F., Courtellemont, T., Pascolutti, R., Seveno, M., Barral, Y. and Piatti, S.** (2015). Rho1- and Pkc1-dependent phosphorylation of the F-BAR protein Syp1 contributes to septin ring assembly. *Mol. Biol. Cell* **26**, 3245-3262. doi:10.1091/mbc.e15-06-0366

**Momany, M., Westfall, P. J. and Abramowsky, G.** (1999). Aspergillus nidulans swo mutants show defects in polarity establishment, polarity maintenance and hyphal morphogenesis. *Genetics* **151**, 557-567.

**Mostowy, S. and Cossart, P.** (2012). Septins: the fourth component of the cytoskeleton. *Nat. Rev. Mol. Cell Biol.* **13**, 183-194. doi:10.1038/nrm3284

**Munro, C. A. and Gow, N. A.** (2001). Chitin synthesis in human pathogenic fungi. *Med Mycol* **39** Suppl. 1, 41-53. doi:10.1080/mmy.39.1.41.53

**Munro, C. A., Selvaggini, S., de Bruijn, I., Walker, L., Lenardon, M. D., Gerssen, B., Milne, S., Brown, A. J. and Gow, N. A.** (2007). The PKC, HOG and $Ca^{2+}$ signalling pathways co-ordinately regulate chitin synthesis in Candida albicans. *Mol. Microbiol.* **63**, 1399-1413. doi:10.1111/j.1365-2958.2007.05588.x

**Ni, M., Rierson, S., Seo, J.-A. and Yu, J.-H.** (2005). The pkaB gene encoding the secondary protein kinase A catalytic subunit has a synthetic lethal interaction with pkaA and plays overlapping and opposite roles in Aspergillus nidulans. *Eukaryot. Cell* **4**, 1465-1476. doi:10.1128/EC.4.8.1465-1476.2005

**Nyholm, T. K., Özdirekcan, S. and Killian, J. A.** (2007). How protein transmembrane segments sense the lipid environment. *Biochemistry* **46**, 1457-1465. doi:10.1021/bi061941c

**Oh, Y. and Bi, E.** (2011). Septin structure and function in yeast and beyond. *Trends Cell Biol.* **21**, 141-148. doi:10.1016/j.tcb.2010.11.006

**Onishi, J., Meinz, M., Thompson, J., Curotto, J., Dreikorn, S., Rosenbach, M., Douglas, C., Abruzzo, G., Flattery, A., Kong, L. et al.** (2000). Discovery of novel antifungal (1,3)-beta-D-glucan synthase inhibitors. *Antimicrob. Agents Chemother.* **44**, 368-377. doi:10.1128/AAC.44.2.368-377.2000

**Onyewu, C., Blankenship, J. R., Del Poeta, M. and Heitman, J.** (2003). Ergosterol biosynthesis inhibitors become fungicidal when combined with calcineurin inhibitors against Candida albicans, Candida glabrata, and Candida krusei. *Antimicrob. Agents Chemother.* **47**, 956-964. doi:10.1128/AAC.47.3.956-964.2003

**Orlean, P.** (2012). Architecture and biosynthesis of the Saccharomyces cerevisiae cell wall. *Genetics* **192**, 775-818. doi:10.1534/genetics.112.144485

**Osmond, B. C., Specht, C. A. and Robbins, P. W.** (1999). Chitin synthase III: synthetic lethal mutants and "stress related" chitin synthesis that bypasses the CSD3/CHS6 localization pathway. *Proc. Natl. Acad. Sci. USA* **96**, 11206-11210. doi:10.1073/pnas.96.20.11206

**Pan, F., Malmberg, R. L. and Momany, M.** (2007). Analysis of septins across kingdoms reveals orthology and new motifs. *BMC Evol. Biol.* **7**, 103. doi:10.1186/1471-2148-7-103

**Pancaldi, S., Poli, F., Dall'Olio, G. and Vannini, G. L.** (1984). Morphological anomalies induced by Congo red in Aspergillus niger. *Arch. Microbiol.* **137**, 185-187. doi:10.1007/BF00414540

**Perez, J., Arcones, I., Gomez, A., Casquero, V. and Roncero, C.** (2016). Phosphorylation of Bni4 by MAP kinases contributes to septum assembly during yeast cytokinesis. *FEMS Yeast Res.* **16**, fow060. doi:10.1093/femsyr/fow060

**Pettolino, F. A., Walsh, C., Fincher, G. B. and Bacic, A.** (2012). Determining the polysaccharide composition of plant cell walls. *Nat. Protoc.* **7**, 1590-1607. doi:10.1038/nprot.2012.081

**Popolo, L., Gilardelli, D., Bonfante, P. and Vai, M.** (1997). Increase in chitin as an essential response to defects in assembly of cell wall polymers in the ggp1delta mutant of Saccharomyces cerevisiae. *J. Bacteriol.* **179**, 463-469. doi:10.1128/JB.179.2.463-469.1997

**Ram, A. F., Wolters, A., Ten Hoopen, R. and Klis, F. M.** (1994). A new approach for isolating cell wall mutants in Saccharomyces cerevisiae by screening for

hypersensitivity to calcofluor white. *Yeast* **10**, 1019-1030. doi:10.1002/yea.320100804

**Ram, A. F., Kapteyn, J. C., Montijn, R. C., Caro, L. H., Douwes, J. E., Baginsky, W., Mazur, P., van den Ende, H. and Klis, F. M.** (1998). Loss of the plasma membrane-bound protein Gas1p in Saccharomyces cerevisiae results in the release of beta1,3-glucan into the medium and induces a compensation mechanism to ensure cell wall integrity. *J. Bacteriol.* **180**, 1418-1424. doi:10.1128/JB.180.6.1418-1424.1998

**Ramstedt, B. and Slotte, J. P.** (2006). Sphingolipids and the formation of sterol-enriched ordered membrane domains. *Biochim. Biophys. Acta* **1758**, 1945-1956. doi:10.1016/j.bbamem.2006.05.020

**Rodriguez-Pena, J. M., Garcia, R., Nombela, C. and Arroyo, J.** (2010). The high-osmolarity glycerol (HOG) and cell wall integrity (CWI) signalling pathways interplay: a yeast dialogue between MAPK routes. *Yeast* **27**, 495-502. doi:10.1002/yea.1792

**Roelants, F. M., Torrance, P. D., Bezman, N. and Thorner, J.** (2002). Pkh1 and Pkh2 differentially phosphorylate and activate Ypk1 and Ykr2 and define protein kinase modules required for maintenance of cell wall integrity. *Mol. Biol. Cell* **13**, 3005-3028. doi:10.1091/mbc.e02-04-0201

**Roncero, C. and Duran, A.** (1985). Effect of Calcofluor white and Congo red on fungal cell wall morphogenesis: in vivo activation of chitin polymerization. *J. Bacteriol.* **163**, 1180-1185. doi:10.1128/JB.163.3.1180-1185.1985

**Santos, N. C., Ter-Ovanesyan, E., Zasadzinski, J. A., Prieto, M. and Castanho, M. A.** (1998). Filipin-induced lesions in planar phospholipid bilayers imaged by atomic force microscopy. *Biophys. J.* **75**, 1869-1873. doi:10.1016/S0006-3495(98)77627-1

**Schmidt, M.** (2004). Survival and cytokinesis of Saccharomyces cerevisiae in the absence of chitin. *Microbiology* **150**, 3253-3260. doi:10.1099/mic.0.27197-0

**Scott, P. H. and Lawrence, J. C.Jr** (1998). Attenuation of mammalian target of rapamycin activity by increased cAMP in 3T3-L1 adipocytes. *J. Biol. Chem.* **273**, 34496-34501. doi:10.1074/jbc.273.51.34496

**Shaw, J. A., Mol, P. C., Bowers, B., Silverman, S. J., Valdivieso, M. H., Duran, A. and Cabib, E.** (1991). The function of chitin synthases 2 and 3 in the Saccharomyces cerevisiae cell cycle. *J. Cell Biol.* **114**, 111-123. doi:10.1083/jcb.114.1.111

**Sims, K. J., Spassieva, S. D., Voit, E. O. and Obeid, L. M.** (2004). Yeast sphingolipid metabolism: clues and connections. *Biochem. Cell Biol.* **82**, 45-61. doi:10.1139/o03-086

**Singh, P., Ramachandran, S. K., Zhu, J., Kim, B. C., Biswas, D., Ha, T., Iglesias, P. A. and Li, R.** (2017). Sphingolipids facilitate age asymmetry of membrane proteins in dividing yeast cells. *Mol. Biol. Cell* **28**, 2712-2722. doi:10.1091/mbc.e17-05-0335

**Sio, S. O., Suehiro, T., Sugiura, R., Takeuchi, M., Mukai, H. and Kuno, T.** (2005). The role of the regulatory subunit of fission yeast calcineurin for in vivo activity and its relevance to FK506 sensitivity. *J. Biol. Chem.* **280**, 12231-12238. doi:10.1074/jbc.M414234200

**Sirajuddin, M., Farkasovsky, M., Hauer, F., Kuhlmann, D., Macara, I. G., Weyand, M., Stark, H. and Wittinghofer, A.** (2007). Structural insight into filament formation by mammalian septins. *Nature* **449**, 311-315. doi:10.1038/nature06052

**Soulard, A., Cremonesi, A., Moes, S., Schutz, F., Jeno, P. and Hall, M. N.** (2010). The rapamycin-sensitive phosphoproteome reveals that TOR controls protein kinase A toward some but not all substrates. *Mol. Biol. Cell* **21**, 3475-3486. doi:10.1091/mbc.e10-03-0182

**Sudoh, M., Yamazaki, T., Masubuchi, K., Taniguchi, M., Shimma, N., Arisawa, M. and Yamada-Okabe, H.** (2000). Identification of a novel inhibitor specific to the fungal chitin synthase. Inhibition of chitin synthase 1 arrests the cell growth, but inhibition of chitin synthase 1 and 2 is lethal in the pathogenic fungus Candida albicans. *J. Biol. Chem.* **275**, 32901-32905. doi:10.1074/jbc.M003634200

**Sugiyama, S. and Tanaka, M.** (2019). Distinct segregation patterns of yeast cell-peripheral proteins uncovered by a method for protein segregatome analysis. *Proc. Natl. Acad. Sci. USA* **116**, 8909-8918. doi:10.1073/pnas.1819715116

**Takeo, K.** (1985). A correlation between mode of growth and regional ultrastructure of the plasma membrane of Schizosaccharomyces pombe as revealed by freeze-fracturing before and after filipin treatment. *J. Gen. Microbiol.* **131**, 309-316. doi:10.1099/00221287-131-2-309

**Takizawa, P. A., DeRisi, J. L., Wilhelm, J. E. and Vale, R. D.** (2000). Plasma membrane compartmentalization in yeast by messenger RNA transport and a septin diffusion barrier. *Science* **290**, 341-344. doi:10.1126/science.290.5490.341

**Tanaka, S. and Tani, M.** (2018). Mannosylinositol phosphorylceramides and ergosterol coodinately maintain cell wall integrity in the yeast Saccharomyces cerevisiae. *FEBS J.* **285**, 2405-2427. doi:10.1111/febs.14509

**Tanaka-Takiguchi, Y., Kinoshita, M. and Takiguchi, K.** (2009). Septin-mediated uniform bracing of phospholipid membranes. *Curr. Biol.* **19**, 140-145. doi:10.1016/j.cub.2008.12.030

**Trimble, W. S. and Grinstein, S.** (2015). Barriers to the free diffusion of proteins and lipids in the plasma membrane. *J. Cell Biol.* **208**, 259-271. doi:10.1083/jcb.201410071

**Valadares, N. F., d' Muniz Pereira, H., Ulian Araujo, A. P. and Garratt, R. C.** (2017). Septin structure and filament assembly. *Biophys Rev* **9**, 481-500. doi:10.1007/s12551-017-0320-4

**Valiante, V., Heinekamp, T., Jain, R., Hartl, A. and Brakhage, A. A.** (2008). The mitogen-activated protein kinase MpkA of Aspergillus fumigatus regulates cell wall signaling and oxidative stress response. *Fungal Genet. Biol.* **45**, 618-627. doi:10.1016/j.fgb.2007.09.006

**Valiante, V., Jain, R., Heinekamp, T. and Brakhage, A. A.** (2009). The MpkA MAP kinase module regulates cell wall integrity signaling and pyomelanin formation in Aspergillus fumigatus. *Fungal Genet. Biol.* **46**, 909-918. doi:10.1016/j.fgb.2009.08.005

**Valiante, V., Macheleidt, J., Foge, M. and Brakhage, A. A.** (2015). The Aspergillus fumigatus cell wall integrity signaling pathway: drug target, compensatory pathways, and virulence. *Front. Microbiol.* **6**, 325. doi:10.3389/fmicb.2015.00325

**van Meer, G., Voelker, D. R. and Feigenson, G. W.** (2008). Membrane lipids: where they are and how they behave. *Nat. Rev. Mol. Cell Biol.* **9**, 112-124. doi:10.1038/nrm2330

**Walker, E. H., Pacold, M. E., Perisic, O., Stephens, L., Hawkins, P. T., Wymann, M. P. and Williams, R. L.** (2000). Structural determinants of phosphoinositide 3-kinase inhibition by wortmannin, LY294002, quercetin, myricetin, and staurosporine. *Mol. Cell* **6**, 909-919. doi:10.1016/S1097-2765(05)00089-4

**Walker, L. A., Munro, C. A., de Bruijn, I., Lenardon, M. D., McKinnon, A. and Gow, N. A.** (2008). Stimulation of chitin synthesis rescues Candida albicans from echinocandins. *PLoS Pathog.* **4**, e1000040. doi:10.1371/journal.ppat.1000040

**Wang, S., Liu, X., Qian, H., Zhang, S. and Lu, L.** (2016). Calcineurin and calcium channel CchA coordinate the salt stress response by regulating cytoplasmic $Ca^{2+}$ homeostasis in aspergillus nidulans. *Appl. Environ. Microbiol.* **82**, 3420-3430. doi:10.1128/AEM.00330-16

**Weete, J. D., Abril, M. and Blackwell, M.** (2010). Phylogenetic distribution of fungal sterols. *PLoS ONE* **5**, e10899. doi:10.1371/journal.pone.0010899

**Wiederhold, N. P., Kontoyiannis, D. P., Prince, R. A. and Lewis, R. E.** (2005). Attenuation of the activity of caspofungin at high concentrations against candida albicans: possible role of cell wall integrity and calcineurin pathways. *Antimicrob. Agents Chemother.* **49**, 5146-5148. doi:10.1128/AAC.49.12.5146-5148.2005

**Wu, J. Q., Ye, Y., Wang, N., Pollard, T. D. and Pringle, J. R.** (2010). Cooperation between the septins and the actomyosin ring and role of a cell-integrity pathway during cell division in fission yeast. *Genetics* **186**, 897-915. doi:10.1534/genetics.110.119842

**Wymann, M. P., Bulgarelli-Leva, G., Zvelebil, M. J., Pirola, L., Vanhaesebroeck, B., Waterfield, M. D. and Panayotou, G.** (1996). Wortmannin inactivates phosphoinositide 3-kinase by covalent modification of Lys-802, a residue involved in the phosphate transfer reaction. *Mol. Cell. Biol.* **16**, 1722-1733. doi:10.1128/MCB.16.4.1722

**Yoshimi, A., Miyazawa, K. and Abe, K.** (2016). Cell wall structure and biogenesis in Aspergillus species. *Biosci. Biotechnol. Biochem.* **80**, 1700-1711. doi:10.1080/09168451.2016.1177446

**Yoshimoto, H., Saltsman, K., Gasch, A. P., Li, H. X., Ogawa, N., Botstein, D., Brown, P. O. and Cyert, M. S.** (2002). Genome-wide analysis of gene expression regulated by the calcineurin/Crz1p signaling pathway in Saccharomyces cerevisiae. *J. Biol. Chem.* **277**, 31079-31088. doi:10.1074/jbc.M202718200

**Yun, Y., Liu, Z., Zhang, J., Shim, W.-B., Chen, Y. and Ma, Z.** (2014). The MAPKK FgMkk1 of Fusarium graminearum regulates vegetative differentiation, multiple stress response, and virulence via the cell wall integrity and high-osmolarity glycerol signaling pathways. *Environ. Microbiol.* **16**, 2023-2037. doi:10.1111/1462-2920.12334

**Zhang, J., Kong, C., Xie, H., McPherson, P. S., Grinstein, S. and Trimble, W. S.** (1999). Phosphatidylinositol polyphosphate binding to the mammalian septin H5 is modulated by GTP. *Curr. Biol.* **9**, 1458-1467. doi:10.1016/S0960-9822(00)80115-3

**Zhang, Y., Gao, T., Shao, W., Zheng, Z., Zhou, M. and Chen, C.** (2017). The septins FaCdc3 and FaCdc12 are required for cytokinesis and affect asexual and sexual development, lipid metabolism and virulence in Fusarium asiaticum. *Mol. Plant Pathol.* **18**, 1282-1294. doi:10.1111/mpp.12492

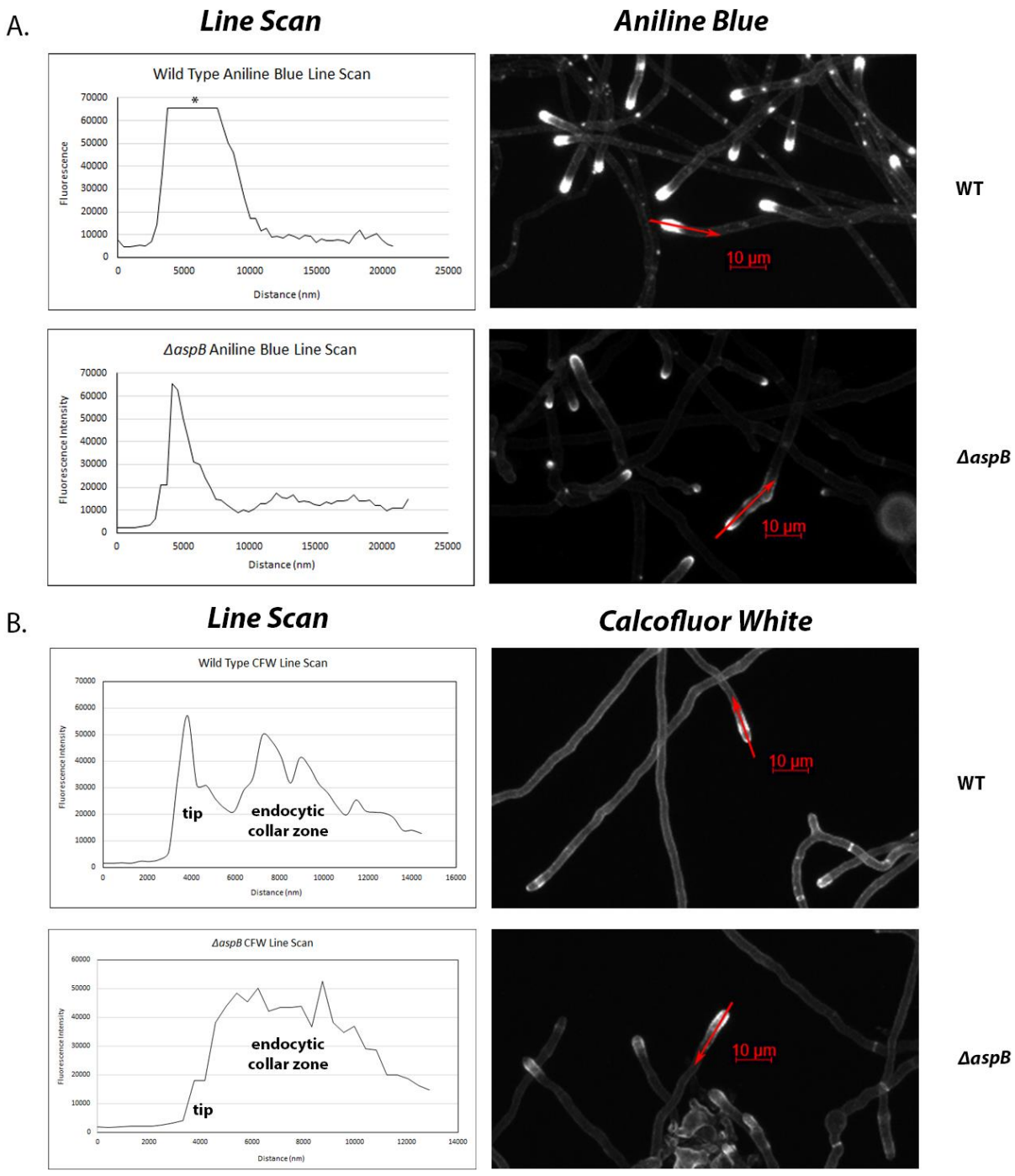


**Fig. S1. Line scans of cell wall staining reveals unique patterns of chitin and β-1,3-glucan deposition in core septin null mutants.** (A) Line scan profiles (Left column) of aniline blue staining patterns, corresponding to the red arrows drawn through the hyphal tips of WT and Δ*aspB*$^{cdc3}$ (Right column). (B) Line scan profiles (Left column) of calcofluor white staining patterns, corresponding to the red arrows drawn through the hyphal tips of WT and Δ*aspB* $^{cdc3}$ (Right column). Asterisk in Panel A line scan profile denotes saturation of fluorescence signal.

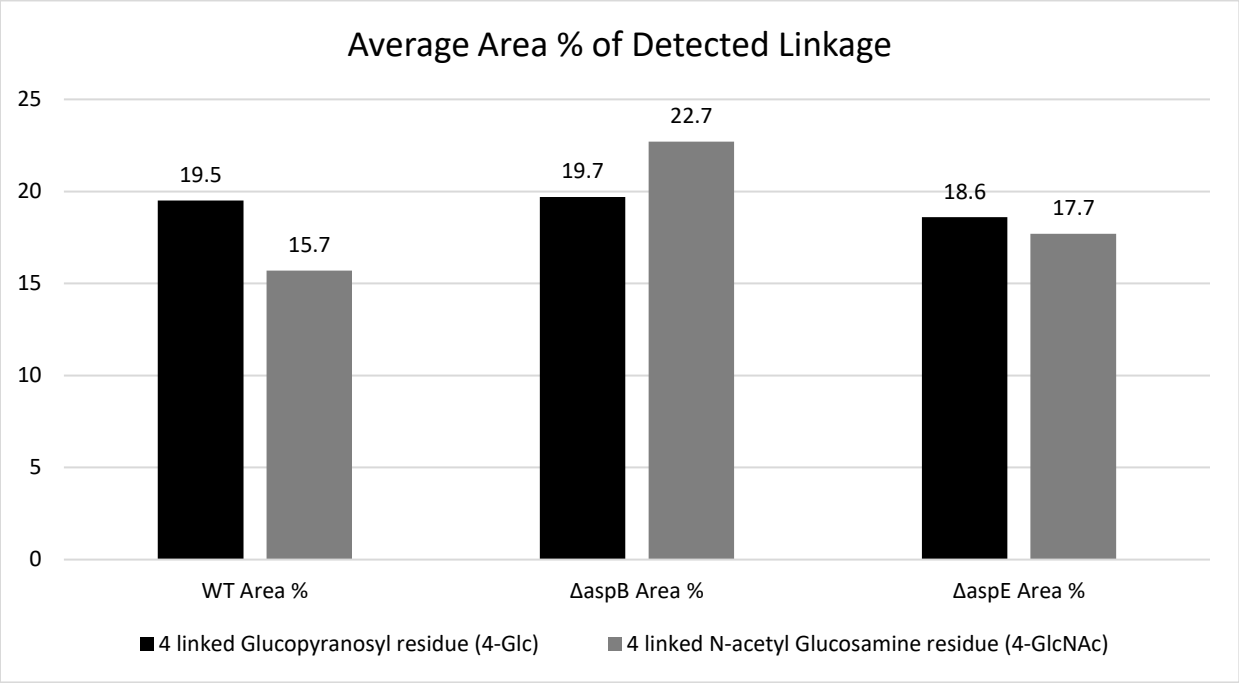


**Fig. S2. Cell wall glycosyl linkage analysis shows increased chitin content in Δ*aspB*$^{cdc3}$ septin null mutant.** Results of cell wall polysaccharide glycosyl linkage analysis using GC MS/MS showing the average area (%) of detected linkages of 4-linked glucose and 4-linked N-acetyl glucosamine. Two independent biological replicates gave similar results. A representative data set is shown. Samples: WT, Δ*aspB*$^{cdc3}$, and Δ*aspE*.

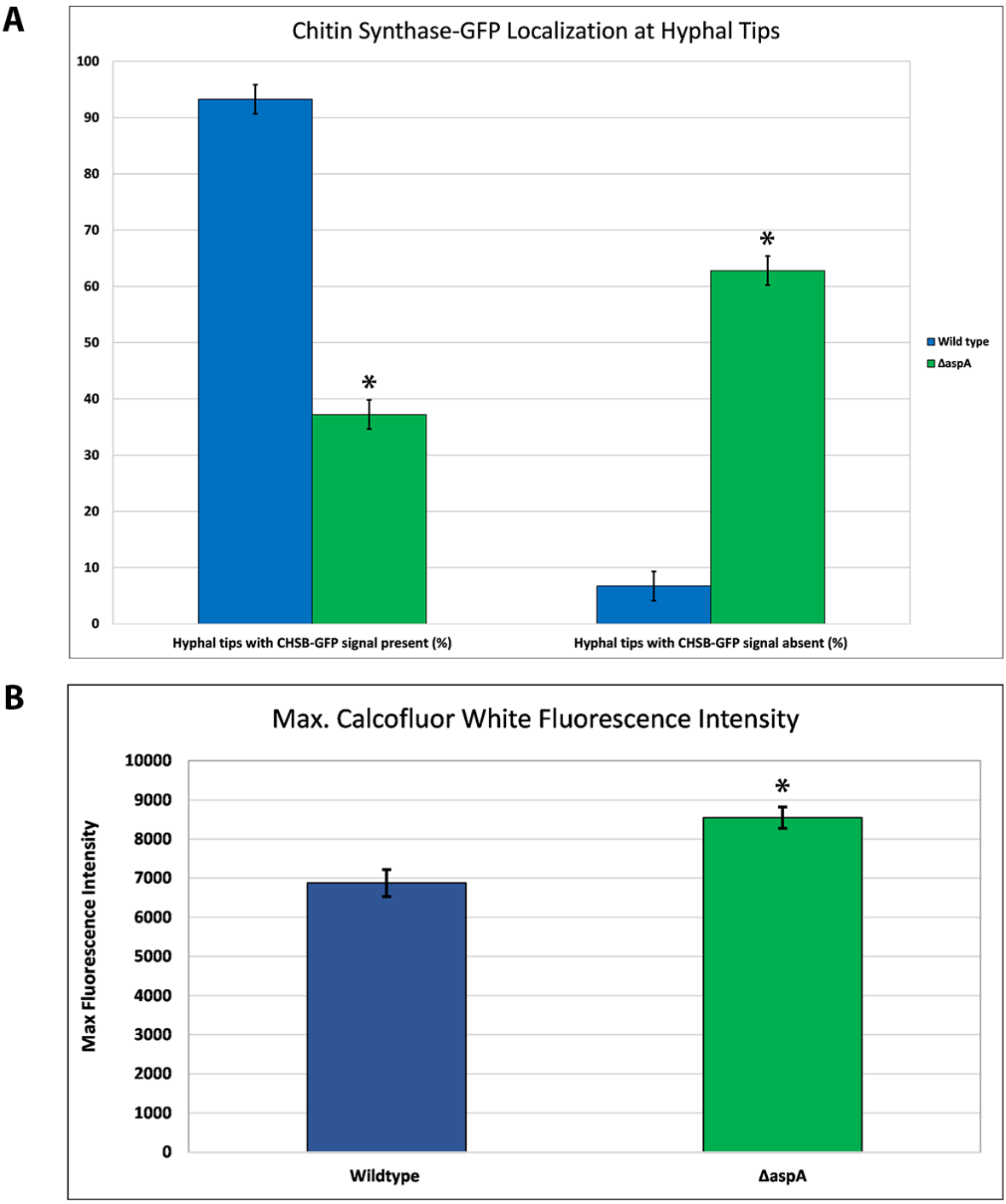


**Fig. S3. Quantification of chitin synthase B-GFP and CFW fluorescence signal. (**A) Quantification of percentage (%) of hyphal branch tips with chitin synthase B-GFP present vs. absent by line scans in WT and Δ*aspA* $^{cdc11}$. Mean values shown for line scans of ≥85 hyphal branches over two independent biological replicates. Asterisks indicate different standard error of the mean between sample sets. (B) Quantification of maximum fluorescence intensity by line scans of CFW stained WT and Δ*aspA* $^{cdc11}$

hyphae (subapical region). Mean values shown for line scans of ≥65 hyphal branches over two independent biological replicates. Asterisks indicate different standard error of the mean between sample sets and statistically different values by two-tailed Ttest ($p < 0.05$) (N=50).

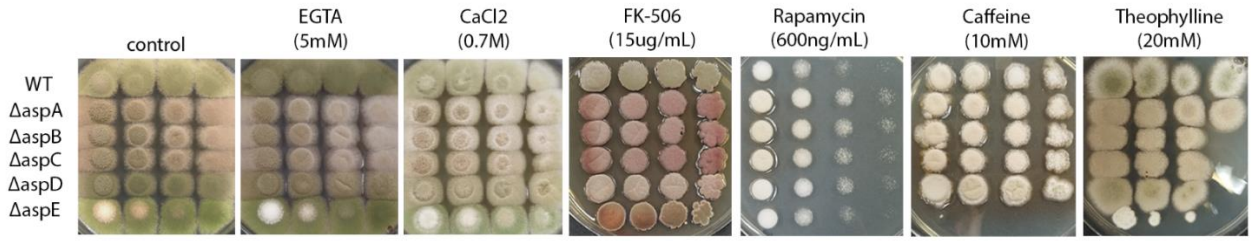


**Fig. S4. Core septin null mutants are not sensitive to treatments which disrupt the Ca2+/ Calcineurin or TOR pathways. AspE is hypersensitive to treatments which disrupt the TOR pathway.** WT and septin null mutants Δ*aspA*$^{cdc11}$, Δ*aspB*$^{cdc3}$, Δ*aspC*$^{cdc12}$, Δ*aspD*$^{cdc10}$, and Δ*aspE* were tested for sensitivity by spotting decreasing spore concentrations on complete media plates with or without Calcium/Calcineurin pathway-disturbing agents (EGTA, CaCl2, and FK-506) or Target of Rapamycin (TOR) pathway-disturbing agents (Rapamycin, caffeine, and theophylline). Differences in colony color result from changes in spore production, spore pigment, and production of secondary metabolites under stress. Spore concentrations were [$1^7$ conidia/mL – $10^4$ conidia/mL] for all assays in figure. N=3

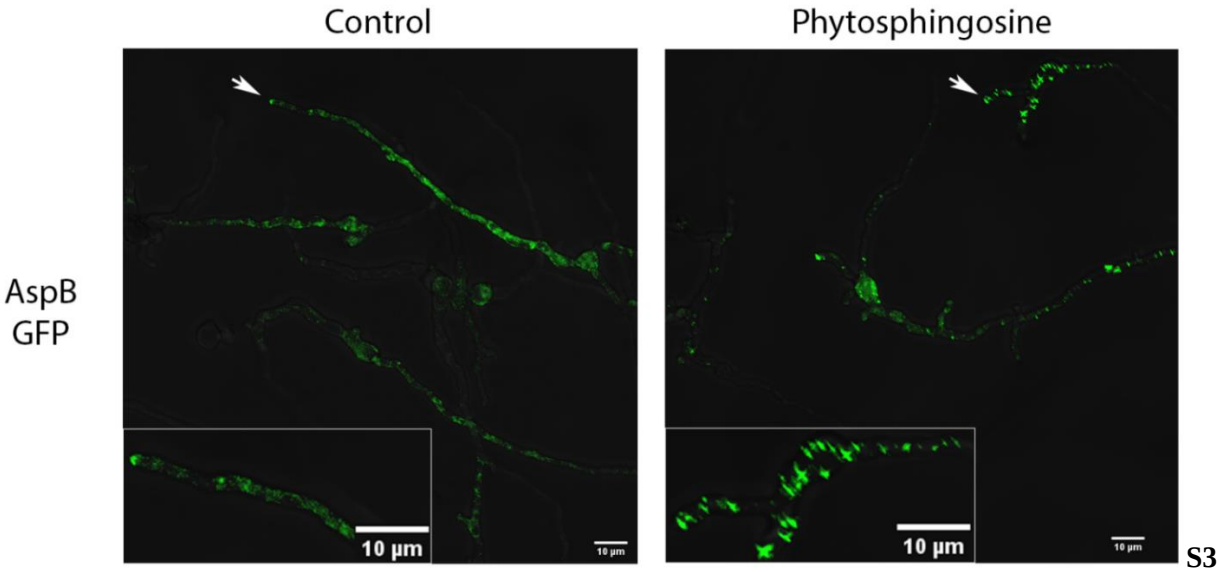


S3

**Fig. S5. Septin AspB$^{Cdc3}$-GFP localization disrupted by sphingolipid biosynthesis intermediate phytosphingosine.** AspB$^{Cdc3}$-GFP strain incubated in liquid media for approximately 16h and imaged 180 minutes after replacing with fresh media containing sphingolipid biosynthesis-inhibiting agents. Representative images are shown from three independent biological replicates, with ≥100 cells observed. (Left Panel) AspB-GFP in vehicle control treatments and (Right Panel) phytosphingosine (15µM) treatment. Enlarged section of micrographs from each picture to better visualize pattern of fluorescence. White arrows denote hyphae which are highlighted in enlarged images. Imaging conducted with Deltavision I deconvolution inverted fluorescence microscope. Scale bars = 10µ m. N=3

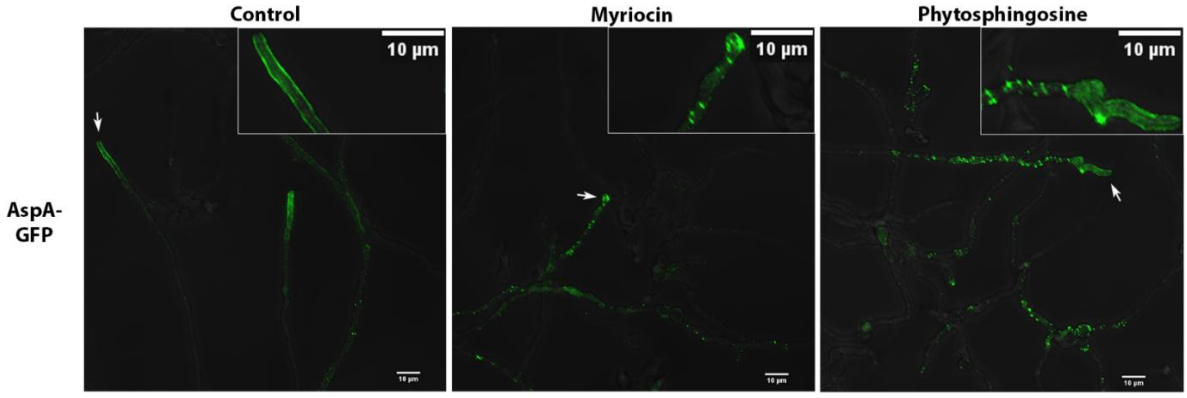


**Fig. S6. Septin AspA$^{Cdc11}$-GFP localization disrupted by sphingolipid biosynthesis inhibitors.** AspA$^{Cdc11}$-GFP strain incubated in liquid media for approximately 16h and imaged 180 minutes after replacing with fresh media containing sphingolipid biosynthesis-inhibiting agents. Representative images are shown from three independent biological replicates, with ≥100 cells observed. (Left Panel) AspA-GFP in vehicle control treatment, (Middle Panel) Myriocin (17.5µg/mL) and (Right Panel) phytosphingosine (15µM) treatment. Enlarged section of micrographs from each picture to better visualize pattern of fluorescence signal. White arrows denote hyphae which are highlighted in enlarged images. Imaging conducted with Deltavision I deconvolution inverted fluorescence microscope. Scale bars = 10µm . N=3

**Table S1.** List of fungal strains used in this study.

| Strain Number | Genotype | Source |
|---|---|---|
| FGSC A850 (WT) | biA1; _argB::trpC_B; methG1; veA1; trpC801 | FGSC |
| ASH5 (Δ*aspA*) | aspA::argB2 biA1 argB::trpC_B methG1 veA1 trpC801 | Lindsey and Momany, 2010 |
| AYR32 (Δ*aspB*) | aspB::AfpyrG; pyroA4; argB2 | Hernandez-Rodriguez et al., 2012 |
| ARL161 (Δ*aspC*) | aspC::AfpyrG pyrG89 biA1 argB::trpC_B methG1 veA1 trpC801 | Lindsey and Momany, 2010 |
| AKK3 (Δ*aspD*) | aspD::AfpyrG; pyroA4; argB2 | Hernandez-Rodriguez et al., 2014 |
| ASH41 (Δ*aspE*) | aspE::AfpyrG; riboB2 | Hernandez-Rodriguez et al., 2012 |
| ANID_05666 (ΔmpkA) | pyrG89; argB2;ΔnkuA(ku70)::argB;ΔmpkA::pyrG;pyroA | CP De Souza et al., 2013 |
| AAM016 (ΔmpkAΔaspB) | aspB::AfpyrG; pyroA4; argB2 + pyrG89; argB2;ΔnkuA(ku70)::argB;ΔmpkA::pyrG;pyroA | This study |
| AAM017 (ΔmpkAΔaspB) | aspB::AfpyrG; pyroA4; argB2+ pyrG89; argB2;ΔnkuA(ku70)::argB;ΔmpkA::pyrG;pyroA | This study |

| | | |
|---|---|---|
| AAM019 (ΔmpkAΔaspE) | aspE::AfpyrG; riboB2+ pyrG89;argB2;ΔnkuA(ku70)::argB;ΔmpkA::pyrG;pyroA | This study |
| AAM020 (ΔmpkAΔaspE) | aspE::AfpyrG; riboB2+ pyrG89; argB2;ΔnkuA(ku70)::argB;ΔmpkA::pyrG;pyroA | This study |
| ARL141 | *aspA-GFP-AfpyrG pyrG89 biA1 argB::trpC_B methG1 veA1 trpC801* | Lindsey and Momany, 2010 |
| EB-5 | *biA1 pyrG89 argB2 pyroA4 wA3 ΔchsB::pyr-4-alcA(p)-chsB argB::chsB(p)-egfp-chsB* | Fukuda et al., 2009 |
| AAM022 | *aspA::argB2 biA1 pyrG89 argB2 wA3 ΔchsB::pyr-4-alcA(p)-chsB argB::chsB(p)-egfp-chsB* | This study |

**Table S2.** List of primers and sequences used in this study.

| Primer Name | Primer Sequence |
|---|---|
| PyrG-Af-R’ | **5’**-CAG AGC CCA CAG AGC GCC TTG AG-**3’** |
| AspB-KO-F’ | **5’**-GGT CAT TCC TGG TGT GAC AGT ACC-**3’** |
| AspE-KO-F’ | **5’**-GAT CCA AAT TCC AGG TTC GAT GAC-**3’** |
| MpkA-806-F’ | **5’**-ATC CTA GAC TCG ACG CCT CA-**3’** |
| MpkA-3779-R’ | **5’**-ACA AAA ACC CCA TCG TCC GA-**3’** |
| AspA-KO-F’ | **5’**-TAG ATC AAG CTC CGC CGG AA-**3’** |
| AspA-KO-R’ | **5’**-TGA CTC CAG CGA CGA TGA GT-**3’** |